bioRxiv preprint doi: https://doi.org/10.1101/2021.02.12.430937; this version posted February 12, 2021. The copyright holder for this preprint (which was not certified by peer review) is the author/funder. All rights reserved. No reuse allowed without permission.

1 **Role of endopeptidases in peptidoglycan synthesis mediated by alternative cross-linking**
2 **enzymes in *Escherichia coli***

3 Henri Voedts[a], Delphine Dorchêne[a], Adam Lodge[b#], Waldemar Vollmer[b], Michel Arthur[a]*, Jean-
4 Emmanuel Hugonnet[a]*

5 [a] Centre de Recherche des Cordeliers, Sorbonne Université, Inserm, Université de Paris, F-75006
6 Paris, France; [b] Centre for Bacterial Cell Biology, Biosciences Institute, Newcastle University,
7 Newcastle Upon Tyne, UK; [#] Present address: Iksuda Therapeutics, The Biosphere, Draymans Way,
8 Newcastle Helix, Newcastle upon Tyne, NE4 5BX, UK.

9 * Corresponding authors, michel.arthur@crc.jussieu.fr; jean-emmanuel.hugonnet@crc.jussieu.fr

10

11 **ABSTRACT**

12 Bacteria resist to the turgor pressure of the cytoplasm through a net-like macromolecule, the
13 peptidoglycan, made of glycan strands connected via peptides cross-linked by penicillin-binding
14 proteins (PBPs). We recently reported the emergence of β-lactam resistance resulting from a
15 bypass of PBPs by the YcbB L,D-transpeptidase (LdtD), which form chemically distinct 3→3 cross-
16 links compared to 4→3 formed by PBPs. Here we show that peptidoglycan expansion requires
17 controlled hydrolysis of cross-links and identify amongst eight endopeptidase paralogues the
18 minimum enzyme complements essential for bacterial growth with 4→3 (MepM) and 3→3
19 (MepM and MepK) cross-links. Purified Mep endopeptidases unexpectedly displayed a 4→3 and
20 3→3 dual specificity implying recognition of a common motif in the two cross-link types.
21 Uncoupling of the polymerization of glycan chains from the 4→3 cross-liking reaction was found
22 to facilitate the bypass of PBPs by YcbB. These results illustrate the plasticity of the peptidoglycan
23 polymerization machinery in response to the selective pressure of β-lactams.

24

bioRxiv preprint doi: https://doi.org/10.1101/2021.02.12.430937; this version posted February 12, 2021. The copyright holder for this preprint (which was not certified by peer review) is the author/funder. All rights reserved. No reuse allowed without permission.

25 **INTRODUCTION**

26 Peptidoglycan (PG) is an essential macromolecule that surrounds the bacterial cell providing
27 resistance to the osmotic pressure of the cytoplasm and determining cell shape (Turner et al.,
28 2014). PG is assembled from a disaccharide-peptide subunit consisting of *N*-acetylglucosamine
29 (GlcNAc) and *N*-acetylmuramic acid (MurNAc) substituted by a stem pentapeptide (L-Ala^1-γ-D-
30 Glu^2-DAP^3-D-Ala^4-D-Ala^5 in which DAP is diaminopimelic acid) (Fig. 1A). The subunit is assembled
31 by glycosyltransferases that polymerize glycan strands and transpeptidases that form amide
32 bonds between stem peptides carried by adjacent glycan strands. *Escherichia coli* relies on two
33 types of transpeptidases for the latter reaction (Magnet et al., 2008). The D,D-transpeptidases,
34 also referred to as penicillin-binding proteins (PBPs), form the most abundant cross-links, which
35 connect the fourth residue (D-Ala^4) of an acyl donor to the third residue (DAP^3) of an acyl acceptor
36 (4→3 cross-link) (Fig. 1A). The L,D-transpeptidases (LDTs) form 3→3 cross-links that connect two
37 DAP residues (Fig. 1B). The D-Ala at the 5th and 4th positions of stem peptides that do not
38 participate in cross-link formation as donors are fully and partially trimmed by carboxypeptidases
39 of the D,D and L,D specificities, respectively (Fig. 1C). PBPs and LDTs are structurally unrelated, rely
40 on different catalytic nucleophiles (Ser *versus* Cys, respectively), and use different acyl donor
41 stems (pentapeptide *versus* tetrapeptide, respectively) (Mainardi et al., 2008; Sauvage et al.,
42 2008). PBPs and LDTs also differ by their inhibition profiles since PBPs are potentially inhibited by
43 all classes of β-lactams (including penams, cephems, monobactams, and carbapenems) whereas
44 LDTs are effectively inhibited only by carbapenems (Mainardi et al., 2005). LDTs are fully
45 dispensable for growth of *E. coli*, at least in laboratory conditions, and form a minority of the
46 cross-links during exponential growth (6% of the total cross-links) (Glauner et al., 1988; Sanders
47 and Pavelka, 2013). The proportion of 3→3 cross-links is higher in the stationary phase (Pisabarro
48 et al., 1985) and in cells experiencing outer membrane assembly stress (Morè et al., 2019). By-
49 pass of PBPs by LDTs leads to high-level resistance to β-lactams of the penam (such as ampicillin),
50 cephem (ceftriaxone), and monobactam (aztreonam) classes in engineered *E. coli* strains that
51 overproduce the YcbB L,D-transpeptidase, also referred to as LdtD, and the guanosine penta- and
52 tetra-phosphate [(p)ppGpp] alarmones (Hugonnet et al., 2016). PG of such strains grown in the

bioRxiv preprint doi: https://doi.org/10.1101/2021.02.12.430937; this version posted February 12, 2021. The copyright holder for this preprint (which was not certified by peer review) is the author/funder. All rights reserved. No reuse allowed without permission.

53 presence of β-lactams exclusively contains 3→3 cross-links, indicating that the D,D-transpeptidase
54 activity of PBPs is fully replaced by the L,D-transpeptidase activity of LDTs.

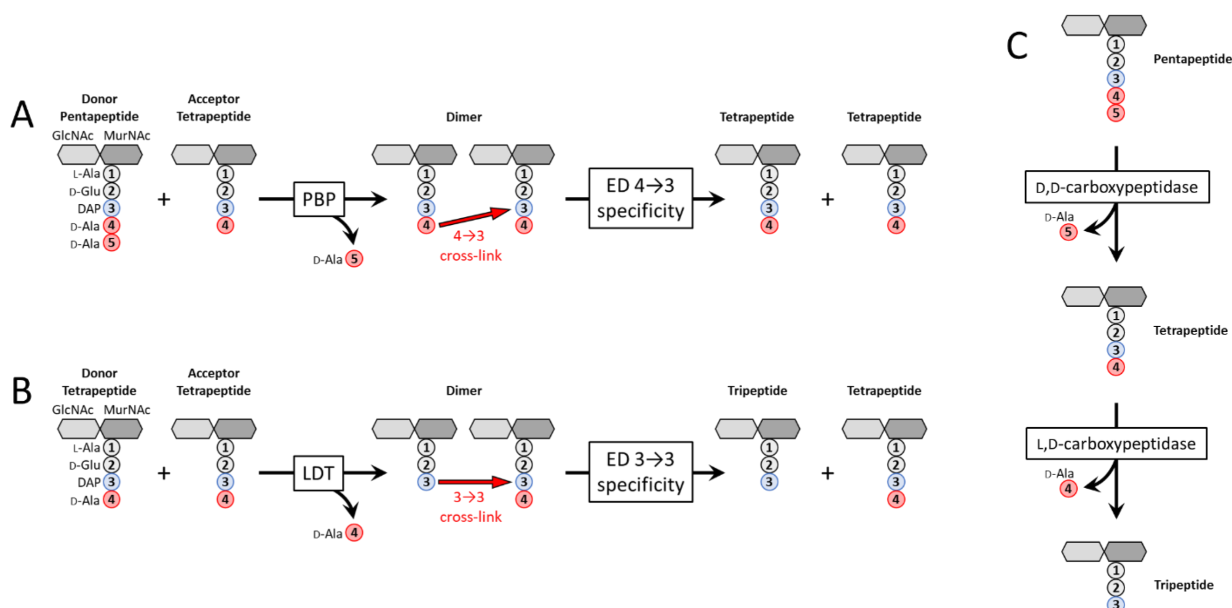

55

56 **Figure 1. Metabolism of PG cross-links and maturation of free stem peptides.** Formation and hydrolysis
57 of (**A**) 4→3 and (**B**) 3→3 crosslinks. The disaccharide-pentapeptide unit is assembled from *N*-
58 acetylglucosamine (GlcNAc), *N*-acetylmuramic acid (MurNAc), and five amino acids including *meso*-
59 diaminopimelic acid (DAP), which is linked via its L (S) center to the γ-carboxyl group of D-Glu. (**C**) Hydrolysis
60 of the D-Ala^4-D-Ala^5 and DAP^3-D-Ala^4 peptide bonds by carboxypeptidases of D,D and L,D specificities,
61 respectively.

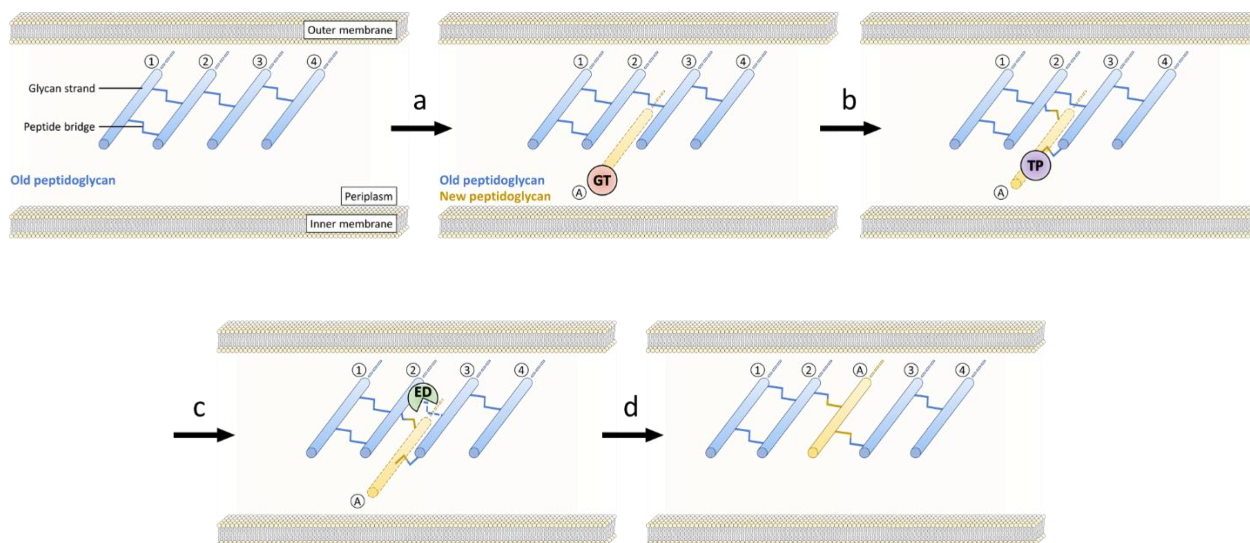

62

63 **Figure S1. Insertion of PG subunits into the growing PG network.** According to this model, one glycan
64 strand (A) is polymerized by glycosyltransferases (GTs; step a) and attached to the pre-existing polymer
65 (strands 2 and 3) by transpeptidases (TPs; step b). Hydrolysis of the cross-links connecting strands 2 and 3
66 by endopeptidases (EDs; step c) results in the expansion of the PG layer (step d). Of note, this model, which

bioRxiv preprint doi: https://doi.org/10.1101/2021.02.12.430937; this version posted February 12, 2021. The copyright holder for this preprint (which was not certified by peer review) is the author/funder. All rights reserved. No reuse allowed without permission.

67 applies to the synthesis of the lateral wall, accounts for incorporation of new subunits sheltered from the
68 cytoplasm osmotic pressure.

69 Expansion of PG is thought to require highly regulated hydrolytic activities that spatially
70 control the insertion of new subunits into the growing network of cross-linked glycan strands
71 (Singh et al., 2012; Vollmer, 2012). Due to the covalent net-like structure of PG, endopeptidases
72 are predicted to be required for insertion of new subunits leading to the expansion of the PG layer
73 (supplementary Fig. S1) (Höltje and Heidrich, 2001). The *E. coli* genome encodes eight
74 endopeptidase paralogues that belong to five enzyme families (Chodisetti and Reddy, 2019; Pazos
75 and Peters, 2019; Singh et al., 2012). PBP4, PBP7, and AmpH belong to the acyl-serine transferase
76 superfamily, which also comprises D,D-transpeptidases and D,D-carboxypeptidases. Members of
77 this superfamily are inhibited by β-lactam antibiotics. The NIpC/P60 cysteine peptidase family
78 comprises two paralogues (MepH and MepS). Metallo-enzymes are represented by three enzyme
79 families, LAS metallopeptidases, lysostaphin/M23 peptidases, and M15 peptidases, each
80 contributing one paralogue (MepA, MepM, and MepK, respectively). The specificity of these eight
81 paralogues as endopeptidases or carboxypeptidases (Fig. 1) has been explored by using sacculi or
82 purified PG fragments as substrates (Chodisetti and Reddy, 2019; Engel et al., 1992; Gonzalez-
83 Leiza et al., 2011; Keck and Schwarz, 1979; Korat et al., 1991; Romeis and Holtje, 1994; Singh et
84 al., 2012). PBP4, PBP7, AmpH, MepH, and MepS hydrolyze 4→3 cross-links but PG dimers
85 containing 3→3 cross-links were not tested. In contrast, MepA, MepM, and MepK were fully
86 characterized revealing that MepA hydrolyzes both 4→3 and 3→3 cross-links, MepM is specific
87 to 4→3 cross-links, and MepK displays a marked preference for 3→3 cross-links. The
88 endopeptidases of *E. coli* are redundant and their essential roles can only be revealed by
89 introducing multiple chromosomal deletions. One study unambiguously showed that hydrolysis
90 of 4→3 cross-links by endopeptidases is essential as the triple deletion of genes encoding MepH,
91 MepM, and MepS was not compatible with growth of *E. coli* in laboratory conditions (Singh et al.,
92 2012; comment by Vollmer, 2012). Several endopeptidases interact genetically and physically
93 with the outer membrane anchored adaptor protein NlpI supporting overlapping functions during
94 the cell cycle (Banzhaf et al., 2020).

bioRxiv preprint doi: https://doi.org/10.1101/2021.02.12.430937; this version posted February 12, 2021. The copyright holder for this preprint (which was not certified by peer review) is the author/funder. All rights reserved. No reuse allowed without permission.

95 The dual capacity of *E. coli* to use transpeptidases of the D,D and L,D specificities raises the
96 possibility that polymerization of PG containing 4→3 or 3→3 cross-links involves two overlapping
97 sets of endopeptidases. To address this question, we used an *E. coli* strain that conditionally and
98 exclusively relies on the formation of 3→3 cross-links for growth in the presence of ampicillin or
99 ceftriaxone (Hugonnet et al., 2016). By introducing serial deletions of endopeptidase genes, we
100 showed that the 4→3 and 3→3 modes of PG polymerization both require hydrolysis of cross-links.
101 We identified distinct sets of endopeptidases that are essential for growth involving the two
102 modes of PG cross-linking. Strikingly, impaired digestion of nascent glycan strands by a lytic
103 transglycosylase was found to favor PG polymerization mediated by LDTs. These results highlight
104 the functional plasticity of PG polymerization complexes to accommodate various PG cross-linking
105 enzymes and hydrolases.

bioRxiv preprint doi: https://doi.org/10.1101/2021.02.12.430937; this version posted February 12, 2021. The copyright holder for this preprint (which was not certified by peer review) is the author/funder. All rights reserved. No reuse allowed without permission.

106 **RESULTS**

107 **MepM is essential for β-lactam resistance mediated by the YcbB L,D-transpeptidase**

108 The role of endopeptidases was assessed in *E. coli* BW25113 Δ*relA* pKT2(*ycbB*) pKT8(*relA'*),
109 BW25113(*ycbB*, *relA'*) in short, which enables controlling the relative contribution of formation
110 of 4→3 and 3→3 cross-links to PG polymerization (Hugonnet et al., 2016). In this strain, the *ycbB*
111 L,D-transpeptidase gene carried by plasmid pKT2 is expressed under the control of an IPTG-
112 inducible promoter. Plasmid pKT8 carries an L-arabinose-inducible copy of the *relA'* gene
113 encoding a truncated version of RelA (residues 1 to 455), which synthesizes the (p)ppGpp
114 alarmone in an unregulated manner due to the absence of the C-terminal ribosome binding
115 module (Schreiber et al., 1991). In the presence of both inducers, production of YcbB and RelA' is
116 sufficient for full bypass of the D,D-transpeptidase activity of PBPs by the L,D-transpeptidase
117 activity of YcbB (Fig. 2A). This enables bacterial growth in the presence of ampicillin or ceftriaxone
118 since these drugs do not inhibit the YcbB L,D-transpeptidase. Testing for the inducible expression
119 of β-lactam resistance in BW25113(*ycbB*, *relA'*) therefore provides a means to identify genes that
120 are essential for growth when PG cross-linking is exclusively mediated by the YcbB L,D-
121 transpeptidase. We used this phenotypic assay to assess the individual role of seven of the eight
122 endopeptidases of *E. coli* following single-gene deletions in the BW25113(*ycbB*, *relA'*) strain (Fig.
123 2B). The remaining endopeptidase MepK could not be tested by this approach since deletion of
124 the corresponding gene was not compatible with the presence of plasmid pKT2(*ycbB*) (see below).
125 Mutants with deletion of *mepA*, *mepH*, *dacB*, *pbpG*, or *ampH* were resistant to ceftriaxone.
126 Deletion of *mepS* decreased plating efficiency in the presence of the drug. Deletion of *mepM*
127 abolished expression of β-lactam resistance. These results are surprising since MepM and MepS
128 were not reported to hydrolyze 3→3 cross-links (Chodisetti and Reddy, 2019; Singh et al., 2012).

bioRxiv preprint doi: https://doi.org/10.1101/2021.02.12.430937; this version posted February 12, 2021. The copyright holder for this preprint (which was not certified by peer review) is the author/funder. All rights reserved. No reuse allowed without permission.

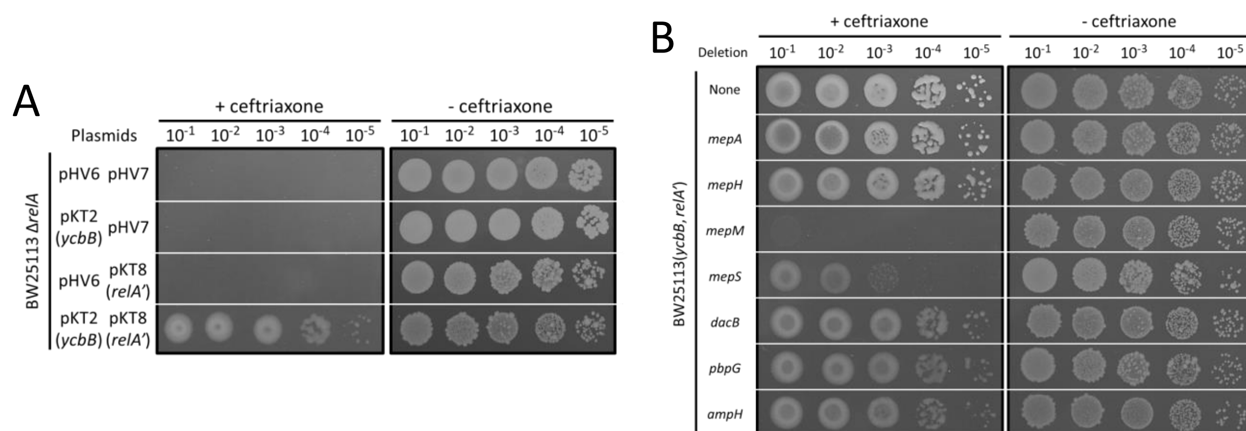

129

130 **Figure 2. MepM is essential for YcbB-mediated β-lactam resistance.** Growth was tested in the presence
131 of ceftriaxone at 8 µg/ml (+ ceftriaxone) or in the absence of the drug (- ceftriaxone) on BHI agar plates
132 supplemented with 40 µM IPTG and 1% L-arabinose for induction of *ycbB* and *relA′*, respectively. (**A**)
133 BW25113 Δ*relA* derivatives harboring plasmids pKT2(*ycbB*), pKT8(*relA′*) and the vectors pHV6 and pHV7
134 used to construct these plasmids, respectively. Expression of β-lactam resistance requires induction of
135 both *ycbB* and *relA′*. (**B**) BW25113(*ycbB*, *relA′*) and its derivatives obtained by individual deletion of
136 endopeptidase genes. BW25113(*ycbB*, *relA′*) is an abbreviated name for BW25113 Δ*relA* pKT2(*ycbB*)
137 pKT8(*relA′*).

138

139 **Production of YcbB is lethal in the absence of MepK**

140 The gene encoding MepK, an endopeptidase with the dual 4→3 and 3→3 specificities was readily
141 deleted from the chromosome of BW25113 Δ*relA*. The resulting strain, BW25113 Δ*relA* Δ*mepK*
142 was transformed with pKT2(*ycbB*), pKT8(*relA′*), or both plasmids in combination (co-
143 transformation). Tetracycline and chloramphenicol were used to select transformants that
144 acquired pKT2(*ycbB*) and pKT8(*relA′*), respectively. Plasmid pKT8(*relA′*) was readily introduced
145 into BW25113 Δ*relA* Δ*mepK* by transformation (10^8 transformants per µg of DNA). Plasmid
146 pKT2(*ycbB*) alone or in combination with pKT8(*relA′*) could not be introduced into BW25113 Δ*relA*
147 Δ*mepK* (< 5 transformants per µg of DNA). The same plating efficacies were observed in selective
148 media containing IPTG, L-arabinose, or both inducers, in addition to tetracycline and
149 chloramphenicol. These results show that production of the YcbB L,D-transpeptidase is lethal in
150 the absence of MepK, in agreement with a recent report (Chodisetti and Reddy, 2019). Thus,
151 cleavage of 3→3 cross-links by MepK is essential for bacterial growth when the proportion of 3→3
152 cross-links is increased in the presence of a plasmid copy of *ycbB*. Quantitatively, the basal level
153 of *ycbB* expression in the absence of IPTG was sufficient for the lethal phenotype associated with

bioRxiv preprint doi: https://doi.org/10.1101/2021.02.12.430937; this version posted February 12, 2021. The copyright holder for this preprint (which was not certified by peer review) is the author/funder. All rights reserved. No reuse allowed without permission.

154 the *mepK* deletion. Under non-inducing conditions the relative proportion of 4→3 and 3→3 cross-
155 links in the PG extracted from exponential phase cultures of BW25113(*ycbB*, *relA'*) was in the
156 order of 60% and 40%, respectively (data not shown). Thus, the cleavage of 3→3 cross-links by
157 MepK was essential even if these cross-links co-existed with 4→3 cross-links formed by the PBPs.

158

159 **The hydrolytic activity of MepM is essential for β-lactam resistance**

160 Deletion of the *mepM* gene abolished YcbB-mediated β-lactam resistance (above, Fig. 2B) even
161 though this endopeptidase was not reported to cleave 3→3 cross-links (Chodisetti and Reddy,
162 2019; Singh et al., 2012). We therefore considered the possibility that the essential role of *mepM*
163 in resistance could involve an as yet unknown function in addition to its 4→3-endopeptidase
164 activity. MepM (440 residues) comprises a LytM (lysostaphin/M23 peptidase) domain and a LysM
165 PG-binding domain (Pfam: P0AFS9). Complementation analysis of the *mepM* deletion in
166 BW25113(*ycbB*, *relA'*) was performed with plasmids encoding (i) MepM, (ii) MepM $H^{393}A$
167 harboring an Ala residue at position 393 in place of an essential catalytic His residue conserved in
168 members of the M23 peptidase family, and (iii) MepM ΔLytM lacking the C-terminal
169 endopeptidase catalytic domain (Fig. 3). Expression of β-lactam resistance by BW25113(*ycbB*,
170 *relA'*) Δ*mepM* was only restored by the plasmid harboring an intact copy of the *mepM* gene. Thus,
171 the complementation analysis led to the conclusion that the endopeptidase activity of MepM is
172 essential for YcbB-mediated resistance to β-lactams.

bioRxiv preprint doi: https://doi.org/10.1101/2021.02.12.430937; this version posted February 12, 2021. The copyright holder for this preprint (which was not certified by peer review) is the author/funder. All rights reserved. No reuse allowed without permission.

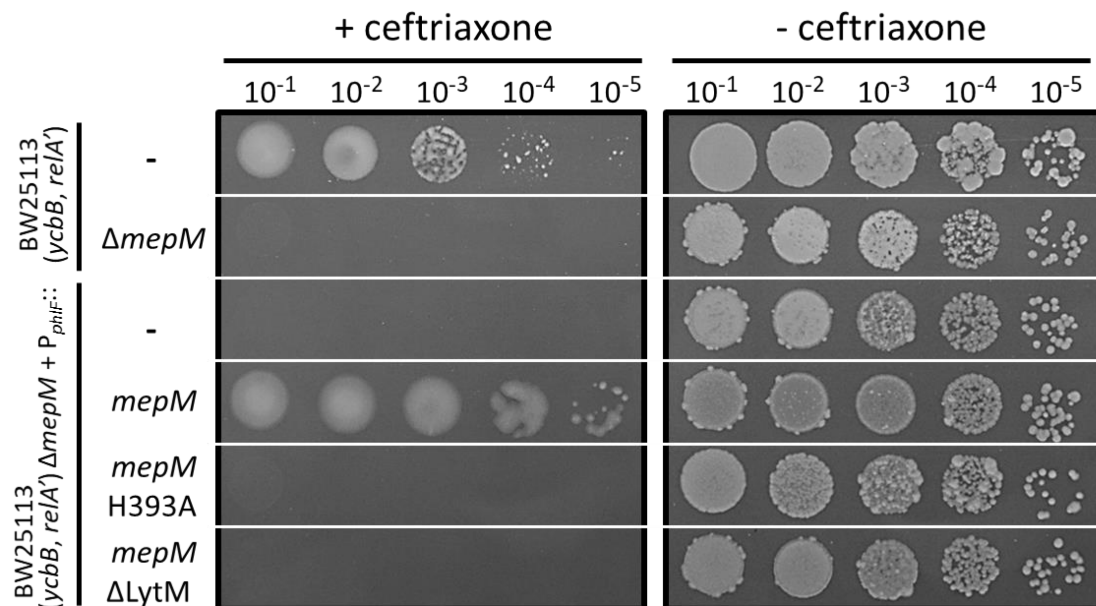

173

174 **Figure 3. MepM endopeptidase activity is required for YcbB-mediated β-lactam resistance.** Growth of
175 BW25113(*ycbB*, *relA'*), BW25113(*ycbB*, *relA'*) Δ*mepM,* and its derivatives harboring plasmids encoding
176 MepM, MepM H^{393}A, and MepM ΔLytM were tested in the presence of ceftriaxone at 8 µg/ml (+
177 ceftriaxone) or in the absence of the drug (- ceftriaxone) in BHI agar plates supplemented with 40 µM IPTG
178 and 1% L-arabinose for induction of *ycbB* and *relA'*, respectively. The genes encoding MepM, MepM H^{393}A,
179 and MepM ΔLytM were inserted into the vector pHV9 under the control of the P_{phlF} promoter, which is
180 inducible by 2,4-diacetylphloroglucinol (DAPG). Basal level of expression of *mepM* under the control of
181 P_{phlF} was sufficient to restore ceftriaxone resistance in the absence of the inducer.

182

183 The essential role of the endopeptidase activity of MepM in β-lactam resistance is not restricted 184 to the transition from 4→3 to 3→3 cross-links triggered by the induction of *ycbB* and *relA'*

185 The experiment reported above did not rule out the possibility that hydrolysis of 4→3 cross-links
186 by MepM might be transiently essential to enable bypass of PBPs by YcbB, *i.e*. cleavage of 4→3
187 cross-links by MepM could be initially essential to enable insertion of new PG subunits into the
188 PG network by YcbB. Ultimately, this would lead to replacement of 4→3 by 3→3 cross-links and
189 could then suppress the essential role of 4→3 cross-link cleavage by MepM. According to this
190 hypothesis, MepM would only be essential during the transition between the two modes of PG
191 cross-linking. To test this possibility, we sought a plasmid construct enabling tight regulation of
192 the *mepM* gene. In a first attempt, *mepM* was cloned under the control of the L-rhamnose-
193 inducible promoter (P_{rhaBAD}) of the pHV30 vector. Complementation of the *mepM* deletion of
194 BW25113(*ycbB*, *relA'*) was obtained both in the presence or absence of L-rhamnose indicating

bioRxiv preprint doi: https://doi.org/10.1101/2021.02.12.430937; this version posted February 12, 2021. The copyright holder for this preprint (which was not certified by peer review) is the author/funder. All rights reserved. No reuse allowed without permission.

195 that the un-induced level of *ycbB* afforded by this plasmid construct was too high (Fig. 4A). To
196 address this issue, the level of *mepM* expression was reduced by replacing the sequence
197 containing the translation initiation signal (TIS1) of *mepM* by a weaker translation initiation signal
198 (TIS2). TIS1 (aAAGAGGAGAAAtgacataATG) combined an ATG initiation codon to a "strong"
199 ribosome-binding-site (RBS) with extensive complementarity (underlined) to the 3' OH extremity
200 of 16S rRNA (5'- AUCACCUCCUUA-3'OH) (Elowitz and Leibler, 2000). TIS2 (acacAGGAcacttaTTG)
201 combined a TTG initiation codon to an RBS with limited complementarity to 16S rRNA (5'-
202 AUCACCUCCUUA-3'OH) (Hecht et al., 2017; Ringquist et al., 1992; Vellanoweth and Rabinowitz,
203 1992). In contrast to the results obtained with TIS1, the presence of L-rhamnose was required for
204 β-lactam resistance if *mepM* was expressed under the control of TIS2 (Fig. 4A). L-rhamnose
205 requirement for growth in the presence of ceftriaxone was not abolished by pre-exposure to the
206 inducer (Fig. 4B). These results indicate that the essential role of MepM in β-lactam resistance is
207 not limited to the transition between the two modes of PG cross-linking, *i.e*. from 4→3 to 3→3.
208 Since all D,D-transpeptidases are inhibited by ceftriaxone, these results also indicate that the
209 hydrolytic activity of MepM is essential in conditions in which 4→3 cross-links are not detectable
210 (Hugonnet et al., 2016; Kocaoglu and Carlson, 2015).

211

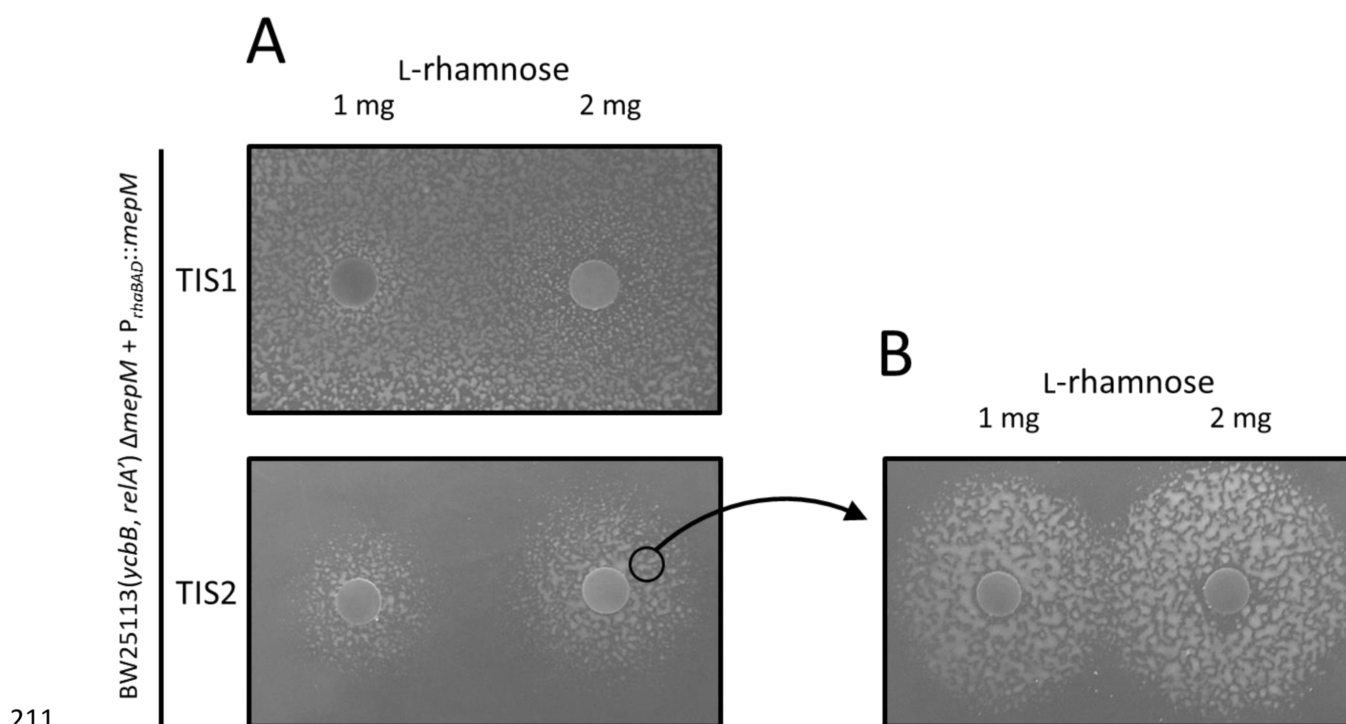

bioRxiv preprint doi: https://doi.org/10.1101/2021.02.12.430937; this version posted February 12, 2021. The copyright holder for this preprint (which was not certified by peer review) is the author/funder. All rights reserved. No reuse allowed without permission.

212 **Figure 4. MepM is essential for β-lactam resistance beyond the transition from 4→3 to 3→3 PG cross-**
213 **linking.** The *mepM* gene was expressed under the control of TIS1 or TIS2 (translation initiation) and of
214 P_{rhaBAD} (the L-rhamnose-inducible promoter of vector pHV30). Growth of BW25113(*ycbB*, *relA'*) Δ*mepM*
215 harboring the pHV30 derivatives was tested on BHI agar supplemented with ceftriaxone 8 µg/ml, IPTG 40
216 µM (induction of *ycbB*) and L-arabinose 1% (induction of *relA'*). (**A**) For TIS2, growth around paper disks
217 containing 1 or 2 mg of L-rhamnose indicated that induction of the expression of *mepM* was required for
218 ceftriaxone resistance. In contrast, a higher level of translation from TIS1 was sufficient for ceftriaxone
219 resistance in the absence of the inducer. (**B**) The experiment was repeated with bacteria pre-exposed to
220 L-rhamnose that were harvested at the vicinity of the disk containing 2 mg of L-rhamnose. Expression of
221 ceftriaxone resistance remained dependent on the presence of L-rhamnose indicating that the
222 requirement for MepM is not transient. The diameter of the growth zones is larger in panel (**B**) than in
223 panel (**A**) as expected from the fact that bacteria in the inoculum used in (**B**) had been grown in the
224 presence of the inducer and already contained MepM. In (**A**) growth is only possible after diffusion of L-
225 rhamnose in the medium prior to the action of ceftriaxone. At a distance from the disk, diffusion was not
226 sufficiently rapid to observe resistance.

227

228 **MepM hydrolyzes both 4→3 and 3→3 cross-links *in vitro***

229 The essential role of the endopeptidase activity of MepM in the context of LDT-mediated PG
230 cross-linking (above) led us to reconsider the specificity of the enzyme. Previous analyses were
231 based on incubation of MepM and lysozyme with an *E. coli* PG preparation containing minute
232 amounts of 3→3 cross-links (Chodisetti and Reddy, 2019; Singh et al., 2012). Analyses of *rp*HPLC
233 profiles revealed that the major dimers containing 4→3 cross-links were digested by MepM but
234 minor peaks corresponding to dimers containing 3→3 cross-links remained unchanged in the
235 presence of the enzyme leading to the conclusion that MepM was specific to 4→3 cross-links
236 (Chodisetti and Reddy, 2019; Singh et al., 2012). To improve the sensitivity of the assay, we
237 purified MepM and reproduced this analysis with a PG preparation of *E. coli* BW25113 grown to
238 stationary phase in minimal medium, which contained a higher proportion of 3→3 cross-links (Fig.
239 5A, upper panel.) The muropeptides corresponding to the indicated peaks are shown in Fig. 5B
240 (see supplementary Fig. S2 for determination of the structure of muropeptides by mass
241 spectrometry). Full digestion of all dimers was observed upon incubation of this PG preparation
242 with MepM (5 µM) indicating that the endopeptidase hydrolyzes both 4→3 and 3→3 cross-links
243 to completion (Fig. 5A, lower panel). Incubation of the PG preparation with lower concentrations
244 of MepM led to partial hydrolysis of the dimers (Fig. 5C). Comparison of the relative abundance
245 of muropeptides based on the integration of peak areas in the chromatograms showed the
246 expected increase in monomers upon digestion of dimers (Fig. 5D). The concentrations of MepM

bioRxiv preprint doi: https://doi.org/10.1101/2021.02.12.430937; this version posted February 12, 2021. The copyright holder for this preprint (which was not certified by peer review) is the author/funder. All rights reserved. No reuse allowed without permission.

247 required for hydrolysis of half of the muropeptides containing 4→3 and 3→3 cross-links were 0.4
248 µM and 0.7 µM, respectively, revealing similar apparent hydrolysis efficacies for the two types of
249 cross-links under the assay conditions (Fig. 5D). These results indicate that hydrolysis of 3→3
250 cross-links may account for the essential role of MepM in conditions in which the L,D-
251 transpeptidase activity of YcbB fully replaces the D,D-transpeptidase activity of the PBPs, as
252 inferred from expression of ceftriaxone resistance by BW25113(*ycbB*, *relA'*) but not by its Δ*mepM*
253 derivative (Fig. 2B).

254 The sum of the relative proportion of tripeptide and tetrapeptide stems in all monomers and
255 dimers did not vary upon addition of MepM (Fig. 5E). This observation indicates that MepM did
256 not hydrolyze D-Ala[4] from tetrapeptide monomers or from tetrapeptide stems located in the
257 acceptor position of dimers. Thus, MepM did not display any L,D-carboxypeptidase activity.

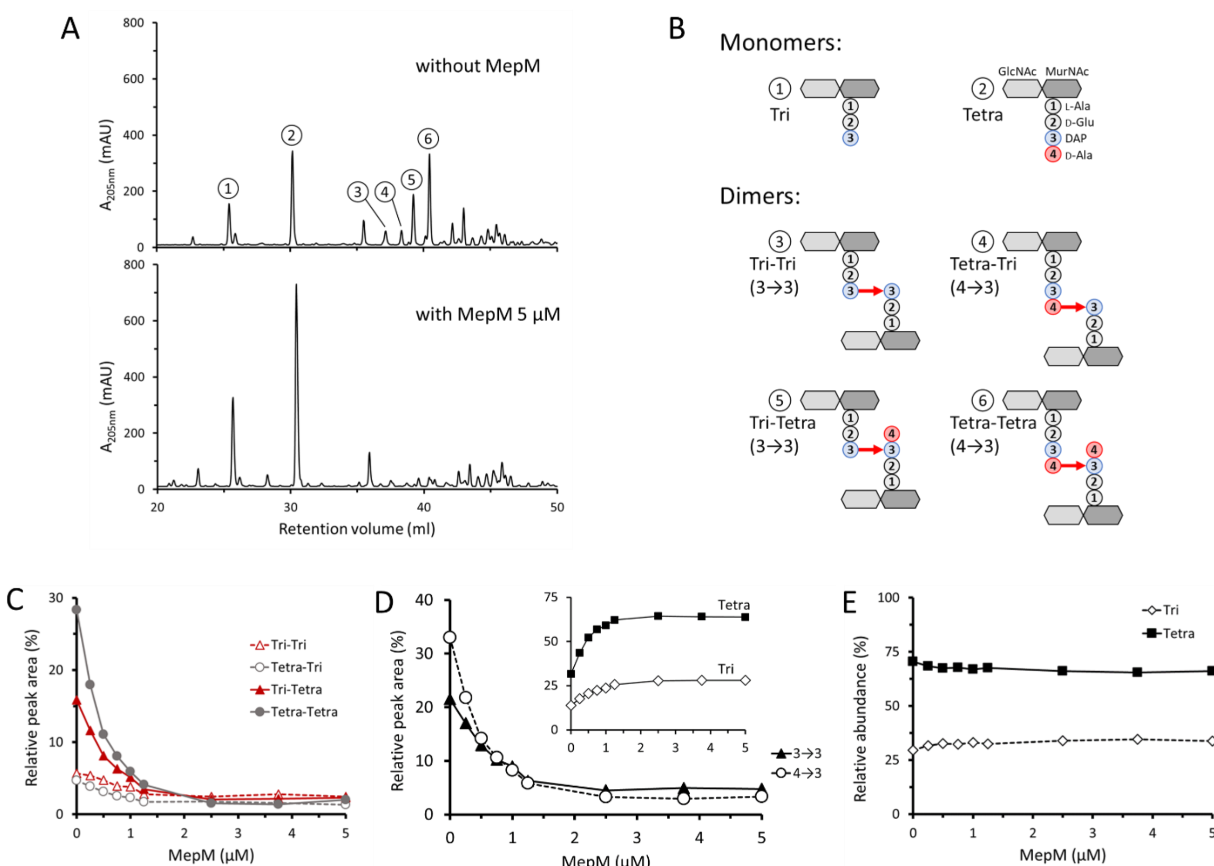

258

259 **Figure 5. Hydrolysis of 4→3 and 3→3 cross-links by purified MepM.** (**A**) *rp*HPLC chromatograms of sacculi
260 isolated from BW25113 grown in minimal medium to stationary phase and digested by lysozyme (upper
261 panel) or by lysozyme and 5 µM MepM (lower panel). Absorbance was monitored at 205 nm (mAU, milli-
262 absorbance unit). (**B**) Structure of the muropeptides as determined by mass spectrometry (supplementary

bioRxiv preprint doi: https://doi.org/10.1101/2021.02.12.430937; this version posted February 12, 2021. The copyright holder for this preprint (which was not certified by peer review) is the author/funder. All rights reserved. No reuse allowed without permission.

263 Fig. S2). (**C**) Hydrolysis of the four types of dimers by MepM. Sacculi were incubated with lysozyme and
264 MepM at various concentrations. The relative abundance of the muropeptides was estimated by
265 calculating the relative peak areas. (**D**) Hydrolysis of dimers containing 4→3 and 3→3 cross-links by MepM.
266 The relative peak areas of Tri-Tri and Tri-Tetra containing 3→3 cross-links and that of Tetra-Tri and Tetra-
267 Tetra containing 4→3 cross-links were combined. The inset shows variations in the relative peak areas of
268 the Tri and Tetra monomers. (**E**) Relative abundance of Tri and Tetra stems in all muropeptides.

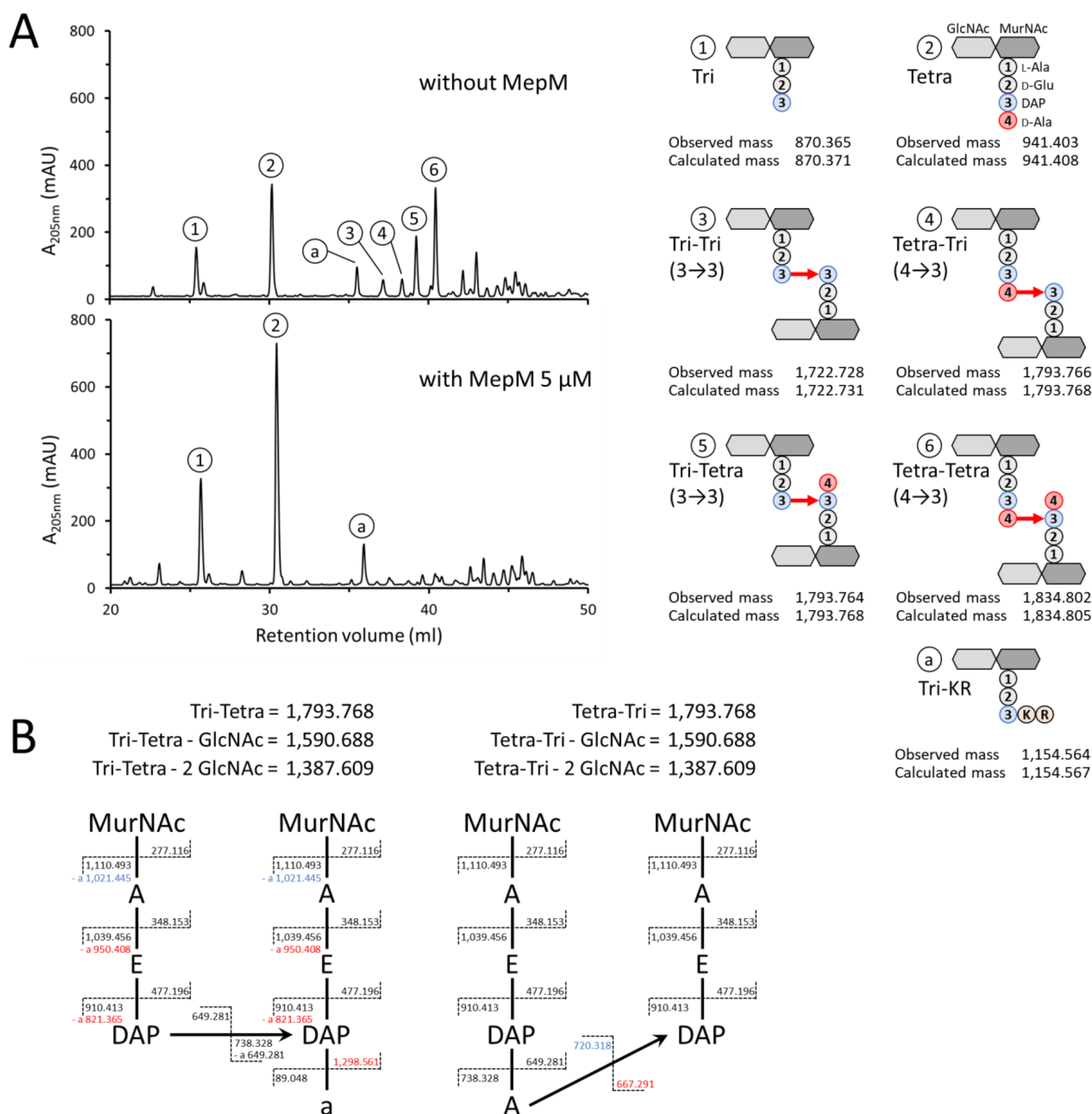

269

270 **Figure S2.** (**A**) Mass spectrometry analysis of muropeptides obtained by digestion of sacculi from BW25113
271 with lysozyme (upper panel) or lysozyme plus MepM (lower panel). The observed and calculated
272 monoisotopic mass are indicated in Dalton. Peak a corresponds to a disaccharide-tripeptide substituted
273 by a Lys-Arg (KR) dipeptide originating from digestion of the covalently-bond Braun lipoprotein by trypsin
274 (Magnet et al., 2008). (**B**) Discrimination of isomers containing 3→3 (Tri-Tetra) and 4→3 (Tetra-Tri) cross-

bioRxiv preprint doi: https://doi.org/10.1101/2021.02.12.430937; this version posted February 12, 2021. The copyright holder for this preprint (which was not certified by peer review) is the author/funder. All rights reserved. No reuse allowed without permission.

275 links by tandem mass spectrometry. All fragments lost both GlcNAc molecules. Fragments that are specific
276 of each isomer are shown in red. Fragments specific of an isomer but which can also be found in the other
277 isomer following loss of a water molecule are shown in blue. Mass of fragments is shown in Dalton. A, L-
278 Ala or D-Ala; a, C-terminal D-Ala; E, D-Glu; DAP, diaminopimelic acid.

279

280 Design of an assay to investigate the redundancy of endopeptidases required for YcbB-281 mediated β-lactam resistance

282 Single deletion of endopeptidase genes revealed four phenotypes (above, Fig. 2B). (i) Deletion of
283 *mepK* was not compatible with production of YcbB. (ii) Deletion of *mepM* abolished YcbB-
284 mediated ceftriaxone resistance. (iii) Deletion of *mepS* impaired growth in the presence of
285 ceftriaxone. (iv) Deletion of *mepA*, *mepH*, *dacB*, *pbpG*, or *ampH* had no impact on growth in the
286 presence of ceftriaxone. The absence of any phenotypic alteration associated with the individual
287 deletion of the latter genes does not necessarily imply that the corresponding endopeptidases
288 are unable to participate in the hydrolysis of 3→3 cross-links. Indeed, the function of these
289 enzymes may be redundant. Alternatively, their level of production may be insufficient under the
290 tested growth conditions. To investigate these possibilities, each of the eight endopeptidase
291 genes was independently cloned under the control of the "strong" TIS1 translation initiation
292 signal downstream from the P_{rhaBAD} promoter of the vector pHV30 in order to modulate the level
293 of endopeptidase production based on induction by L-rhamnose. The plasmids were introduced
294 into BW25113(*ycbB*, *relA'*) Δ*mepM* and growth of the resulting strains was tested in the presence
295 or absence of L-rhamnose and in the presence or absence of ceftriaxone in all combinations (Fig.
296 6).

297

298 Overexpression of *mepM* is toxic in the presence of ceftriaxone

299 The assay described above revealed that the basal level of expression of the plasmid copy of
300 *mepM* in the absence of the inducer was sufficient to restore growth of BW25113(*ycbB*, *relA'*)
301 Δ*mepM* in the presence of ceftriaxone (Fig. 6). Induction of the *mepM* gene by L-rhamnose
302 prevented growth in the presence of ceftriaxone but not in the absence of the drug. These results
303 suggest that overproduction of MepM inhibits growth by cleavage of 3→3 cross-links if 4→3
304 cross-links are absent due to the inactivation of the PBPs by ceftriaxone.

bioRxiv preprint doi: https://doi.org/10.1101/2021.02.12.430937; this version posted February 12, 2021. The copyright holder for this preprint (which was not certified by peer review) is the author/funder. All rights reserved. No reuse allowed without permission.

305

306 **Overexpression of *mepS* complements the *mepM* deletion for expression of YcbB-mediated β-**
307 **lactam resistance**

308 MepS restored growth of BW25113(*ycbB*, *relA'*) Δ*mepM* only in the presence of the inducer (Fig.
309 6). Thus, MepM and MepS have overlapping functions although overproduction of MepS was
310 required to compensate for the absence of MepM. As mentioned above (Fig. 2B), deletion of
311 *mepS* impaired but did not abolish ceftriaxone resistance in BW25113(*ycbB*, *relA'*). Together these
312 results indicate that expression of *mepS* in its native chromosomal environment contributes to
313 resistance but the level of its expression is not sufficient to compensate for the absence of MepM.

314

315 **Partial complementation of the *mepM deletion* by *mepH***

316 The plasmid encoding MepH partially restored growth of BW25113(*ycbB*, *relA'*) Δ*mepM* on
317 ceftriaxone only in the presence of L-rhamnose (Fig. 6). This result indicates that MepH, like MepS,
318 replaces MepM for the expression of ceftriaxone resistance if MepH is overproduced.

319

320 **Purified MepS and MepH hydrolyze 4→3 and 3→3 cross-links (endopeptidase activity) and the**
321 **DAP-D-Ala bond of tetrapeptide stems (L,D-carboxypeptidase activity)**

322 Complementation of Δ*mepM* by overproduction of MepS and MepH prompted us to evaluate the
323 specificity of these enzymes, as described above for MepM. MepH and MepS both hydrolyzed
324 4→3 and 3→3 cross-links (Fig. 7A and B). MepS showed no preference for 4→3 or 3→3 cross-links
325 while MepH displayed a strong preference for 4→3 cross-links. The weak hydrolytic activity of
326 MepH on 3→3 cross-links may account for the fact that the overproduction of MepH can only
327 partially compensate for the absence of MepM (Fig. 6, above). Both MepS and MepH displayed
328 L,D-carboxypeptidase activity leading to rapid conversion of tetrapeptide stems into tripeptide
329 stems (Fig. 7A and B).

330

331 **MepA and MepK do not compensate the absence of MepM**

bioRxiv preprint doi: https://doi.org/10.1101/2021.02.12.430937; this version posted February 12, 2021. The copyright holder for this preprint (which was not certified by peer review) is the author/funder. All rights reserved. No reuse allowed without permission.

332 In spite of the fact that MepA and MepK were previously shown to cleave 3→3 cross-links
333 (Chodisetti and Reddy, 2019; Engel et al., 1992), growth of BW25113(*ycbB*, *relA'*) Δ*mepM* on
334 ceftriaxone was not restored by overproduction of these enzymes (Fig. 6). Thus, there was not a
335 strict correlation between the ability of the endopeptidases to hydrolyze 3→3 cross-links *in vitro*
336 and their ability to restore growth of BW25113(*ycbB*, *relA'*) Δ*mepM*. This absence of correlation
337 was particularly striking for MepK since this endopeptidase, which preferentially hydrolyze 3→3
338 cross-links *in vitro* (Chodisetti and Reddy, 2019), did not complement the *mepM* deletion although
339 it was required for growth of BW25113(*ycbB*, *relA'*) expressing the *ycbB* L,D-transpeptidase gene.

340 These results indicate that functional properties of the endopeptidases, beyond their mere
341 hydrolytic specificity, are relevant to the bypass of the D,D-transpeptidase activity of PBPs by the
342 L,D-transpeptidase activity of YcbB. These properties may include the interaction of the
343 endopeptidases with other proteins that regulate their spatiotemporal activity (see discussion
344 section).

345

346 **Endopeptidases of the PBP family do not compensate the absence of MepM**

347 Complementation of the *mepM* deletion was not observed for PBP4, PBP7, and AmpH both in the
348 presence or absence of induction of the corresponding genes by L-rhamnose (Fig. 6). There is a
349 caveat for these endopeptidases since they are potentially inhibited by ceftriaxone. To address
350 this issue, the complementation test was repeated with ampicillin, cefsulodin, and aztreonam,
351 which were reported to exhibit different selectivities for inhibition of the PBPs (Henderson et al.,
352 1997; Kocaoglu and Carlson, 2015). Plasmids encoding PBP4, PBP7, and AmpH did not restore
353 growth of BW25113(*ycbB*, *relA'*) Δ*mepM* in the presence of ampicillin, cefsulodin, and aztreonam
354 (supplementary Fig. S3) confirming that these endopeptidases are unable to compensate for the
355 absence of MepM. PBP4 and PBP7 were purified and shown to only cleave 4→3 cross-links (Fig.
356 7C and D). Thus, the absence of complementation of the *mepM* deletion by the plasmids encoding
357 these PBPs can be accounted for by their lack of hydrolytic activities on 3→3 cross-linked dimers.
358 PBP4 and PBP7 did not display L,D-carboxypeptidase activity.

bioRxiv preprint doi: https://doi.org/10.1101/2021.02.12.430937; this version posted February 12, 2021. The copyright holder for this preprint (which was not certified by peer review) is the author/funder. All rights reserved. No reuse allowed without permission.

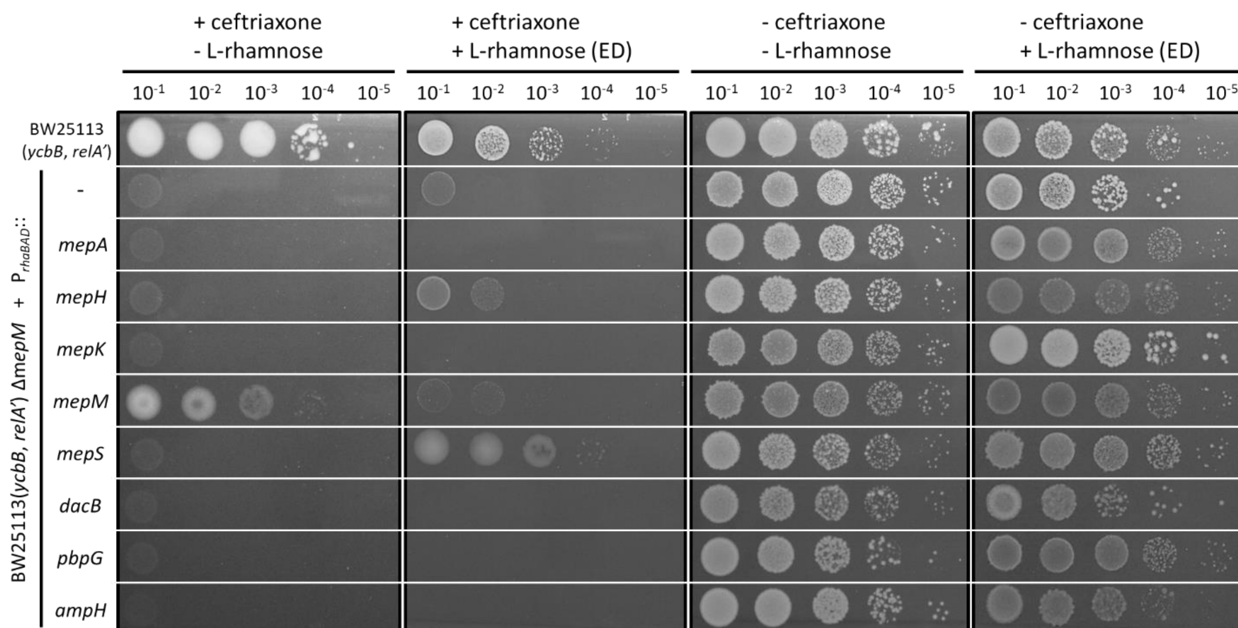

359

360 **Figure 6. Complementation of the *mepM* deletion by plasmids encoding L-rhamnose-inducible copies of**
361 **the eight endopeptidase genes.** Functional complementation of the *mepM* deletion in BW25113(*ycbB*,
362 *relA'*) Δ*mepM* was performed with the pHV30 vector or recombinant plasmids encoding each of the eight
363 endopeptidases under the control of the P_{rhaBAD} promoter. Induction of endopeptidase (ED) genes was
364 performed with 0.2% L-rhamnose in the presence or absence of 8 µg/ml ceftriaxone. BHI agar plates
365 contained 40 µM IPTG and 1% L-arabinose for induction of *ycbB* and *relA'*, respectively.

366

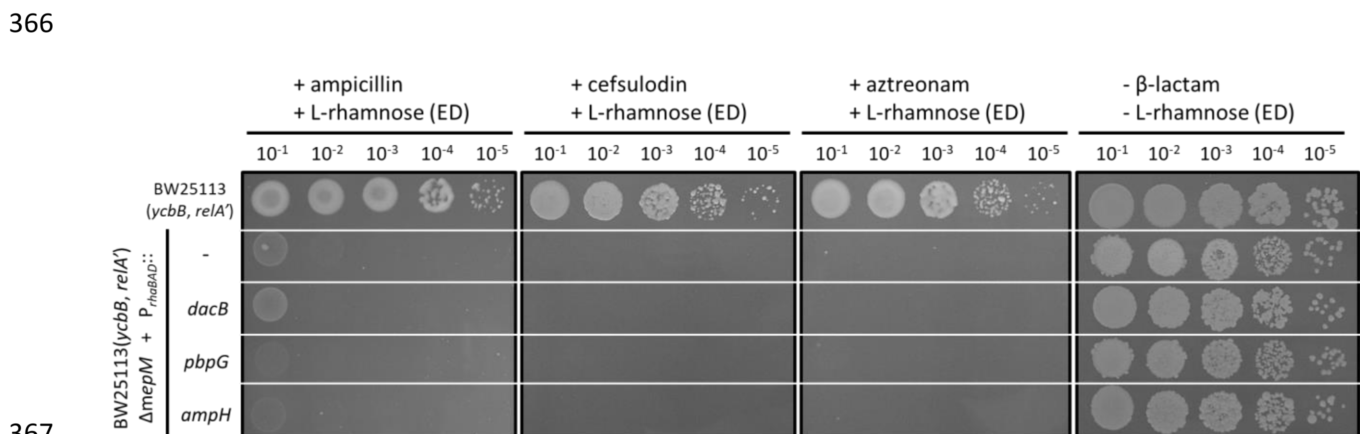

367

368

369 **Figure S3. Complementation of the *mepM* deletion by endopeptidases of the PBP family.** Functional
370 complementation of the *mepM* deletion of BW25113(*ycbB*, *relA'*) Δ*mepM* was performed with the pHV30
371 vector or recombinant plasmids encoding PBP4, PBP7, and AmpH under the control of the P_{rhaBAD}
372 promoter. Induction of endopeptidase (ED) genes was performed with 0.2% L-rhamnose in the presence
373 or absence of 16 µg/ml ampicillin, 32 µg/ml cefsulodin, or 8 µg/ml aztreonam. BHI agar plates contained
374 40 µM IPTG and 1% L-arabinose for induction *ycbB* and *relA'*, respectively.

375

bioRxiv preprint doi: https://doi.org/10.1101/2021.02.12.430937; this version posted February 12, 2021. The copyright holder for this preprint (which was not certified by peer review) is the author/funder. All rights reserved. No reuse allowed without permission.

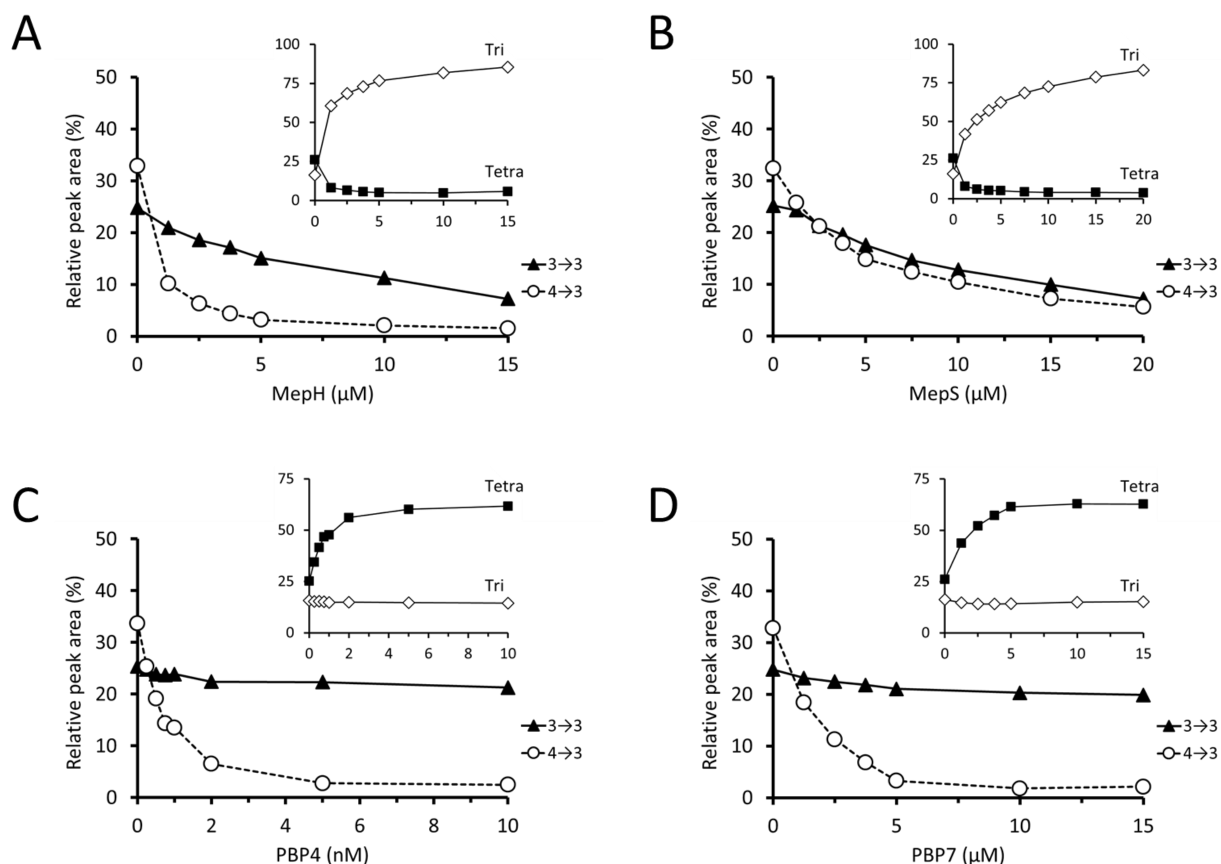

376

377 **Figure 7. Hydrolysis of 4→3 and 3→3 cross-links by purified endopeptidases.** Sacculi were incubated with
378 lysozyme and purified MepH (**A**), MepS (**B**), PBP4 (**C**), and PBP7 (**D**). The relative peak areas of Tri-Tri and
379 Tri-Tetra containing 3→3 cross-links and that of Tetra-Tri and Tetra-Tetra containing 4→3 cross-links were
380 combined. MepH preferentially hydrolyzed dimers containing 4→3 cross-links. MepS hydrolyzed dimers
381 containing 4→3 and 3→3 cross-links with similar efficacies. PBP4 and PBP7 only hydrolyzed dimers
382 containing 4→3 cross-links. The insets show variations in the relative peak areas of the Tri and Tetra
383 monomers. MepH and MepS displayed L,D-carboxypeptidase activity, but not PBP4 and PBP7.

384

385 Minimal complement of endopeptidases required for growth in the context of the formation of 386 4→3 cross-links by PBPs

387 Previous analyses based on multiple deletions showed that genes encoding endopeptidases
388 belonging to the PBP family (PBP4, PBP7, and AmpH) are collectively dispensable (Denome et al.,
389 1999). Independently, deletion of the genes encoding MepH, MepM, and MepS in various
390 combinations revealed that at least one of these endopeptidases was essential (Singh et al.,
391 2012). Here, we extend these analyses to the full complement of the eight endopeptidase genes.

bioRxiv preprint doi: https://doi.org/10.1101/2021.02.12.430937; this version posted February 12, 2021. The copyright holder for this preprint (which was not certified by peer review) is the author/funder. All rights reserved. No reuse allowed without permission.

392 Serial deletions of endopeptidase genes were introduced into the chromosome of *E. coli*
393 BW25113 Δ*relA* generating the lineages depicted in supplementary Fig. S4. This approach
394 culminated in the construction of a viable derivative of BW25113 Δ*relA,* designated Δ7EDs
395 (lineage 5 in supplementary Fig. S4), which retained only one of the eight endopeptidase genes
396 (*mepM*). Thus, MepM alone was necessary and sufficient to support bacterial growth in the
397 context of the 4→3 mode of cross-linking.

398 Our next objective was to determine whether deletion of *mepM* could be complemented by
399 overproduction of other endopeptidases. To address this question, the *mepM* gene was cloned
400 under the L-rhamnose-inducible promoter of vector pHV30 and introduced into the Δ7EDs strain.
401 The chromosomal copy of *mepM* was deleted from the resulting strain leading to strain Δ8EDs
402 pHV53(*mepM*), which was dependent upon the presence of L-rhamnose for growth (Fig. 8A). The
403 plasmids enabling L-arabinose-inducible expression of the eight endopeptidase genes (above)
404 were introduced in the Δ8EDs pHV53(*mepM*) strain to determine which endopeptidase could
405 functionally replace MepM (Fig. 8B). Induction by L-arabinose of the genes encoding MepM,
406 MepH, MepS, and PBP7 suppressed the requirement for L-rhamnose for growth. These results
407 indicate that a single endopeptidase, MepM, MepH, MepS, or PBP7, is potentially sufficient for
408 growth in the context of the 4→3 mode of cross-linking. Except for MepM, this required
409 overproduction of the enzymes following induction of the P_{araBAD} promoter of the recombinant
410 plasmids.

bioRxiv preprint doi: https://doi.org/10.1101/2021.02.12.430937; this version posted February 12, 2021. The copyright holder for this preprint (which was not certified by peer review) is the author/funder. All rights reserved. No reuse allowed without permission.

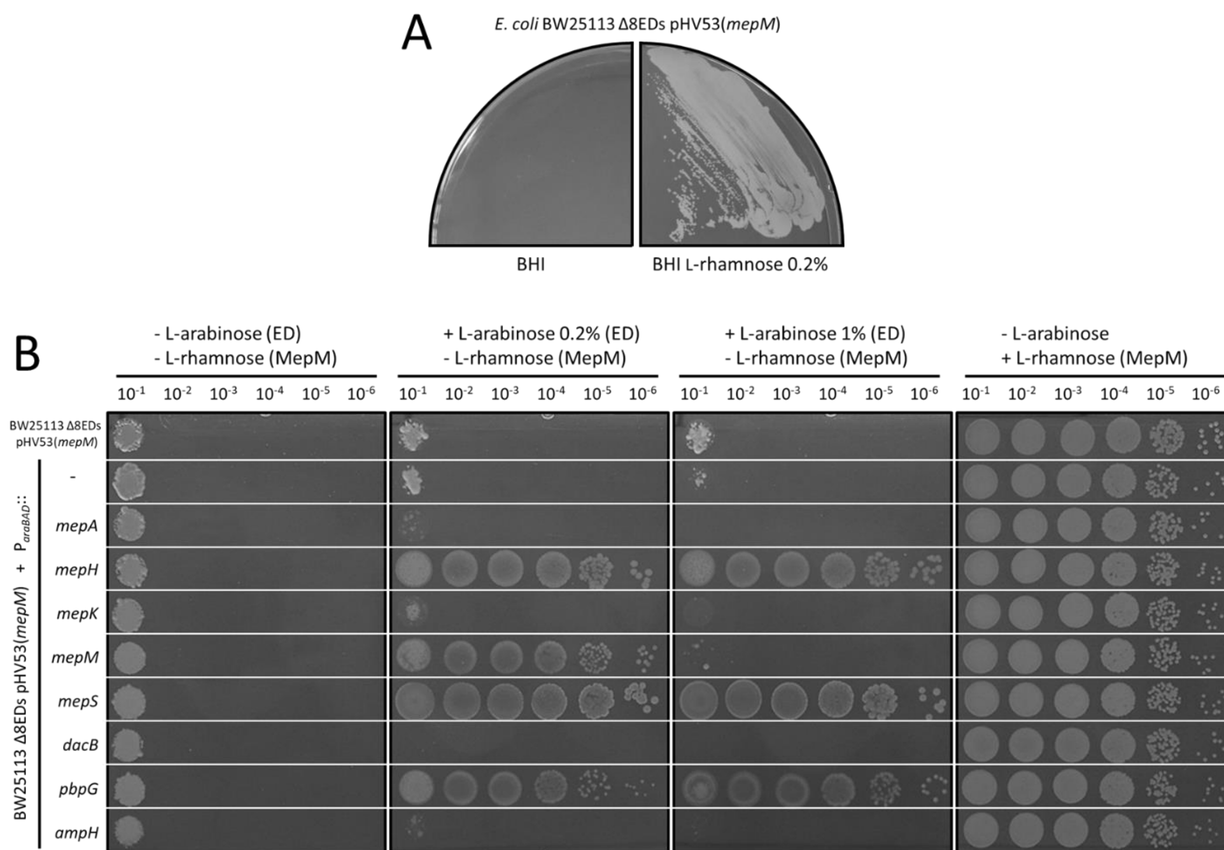

411

412 **Figure 8. Minimal complement of endopeptidases required for growth in the context of the formation of 4→3 cross-links by PBPs.** (**A**) BW25113 Δ8EDs harboring a plasmid carrying the *mepM* gene under the control of the P_{rhaBAD} L-rhamnose-inducible promoter with the "weak" TIS2 translation initiation signal (plasmid pHV53) was grown on BHI agar in the absence or presence of 0.2% L-rhamnose. Growth was dependent upon induction of the *mepM* copy carried by pHV53. (**B**) The plating efficiency assay was performed with derivatives of BW25113 Δ8EDs pHV53(*mepM*) harboring the vector pHV7 or recombinant plasmids carrying each of the eight endopeptidase genes under the control of the P_{araBAD} promoter. In this assay, functional replacement of MepM is detected based on growth in media containing 0.2% or 1% L-arabinose for expression of the endopeptidase gene carried by vector pHV7, while by-passing the requirement for induction of the *mepM* copy of pHV53 by L-rhamnose. Complementation was observed with both concentrations of inducer for *mepH*, *mepS*, and *pbpG*. Overproduction of *mepM* encoded by the pHV7 derivative in the presence of the high dose of L-arabinose (1%) was lethal. The right panel presents the growth control performed in the presence of 0.2% L-rhamnose for induction of the *mepM* copy carried by pHV53.
413–425

bioRxiv preprint doi: https://doi.org/10.1101/2021.02.12.430937; this version posted February 12, 2021. The copyright holder for this preprint (which was not certified by peer review) is the author/funder. All rights reserved. No reuse allowed without permission.

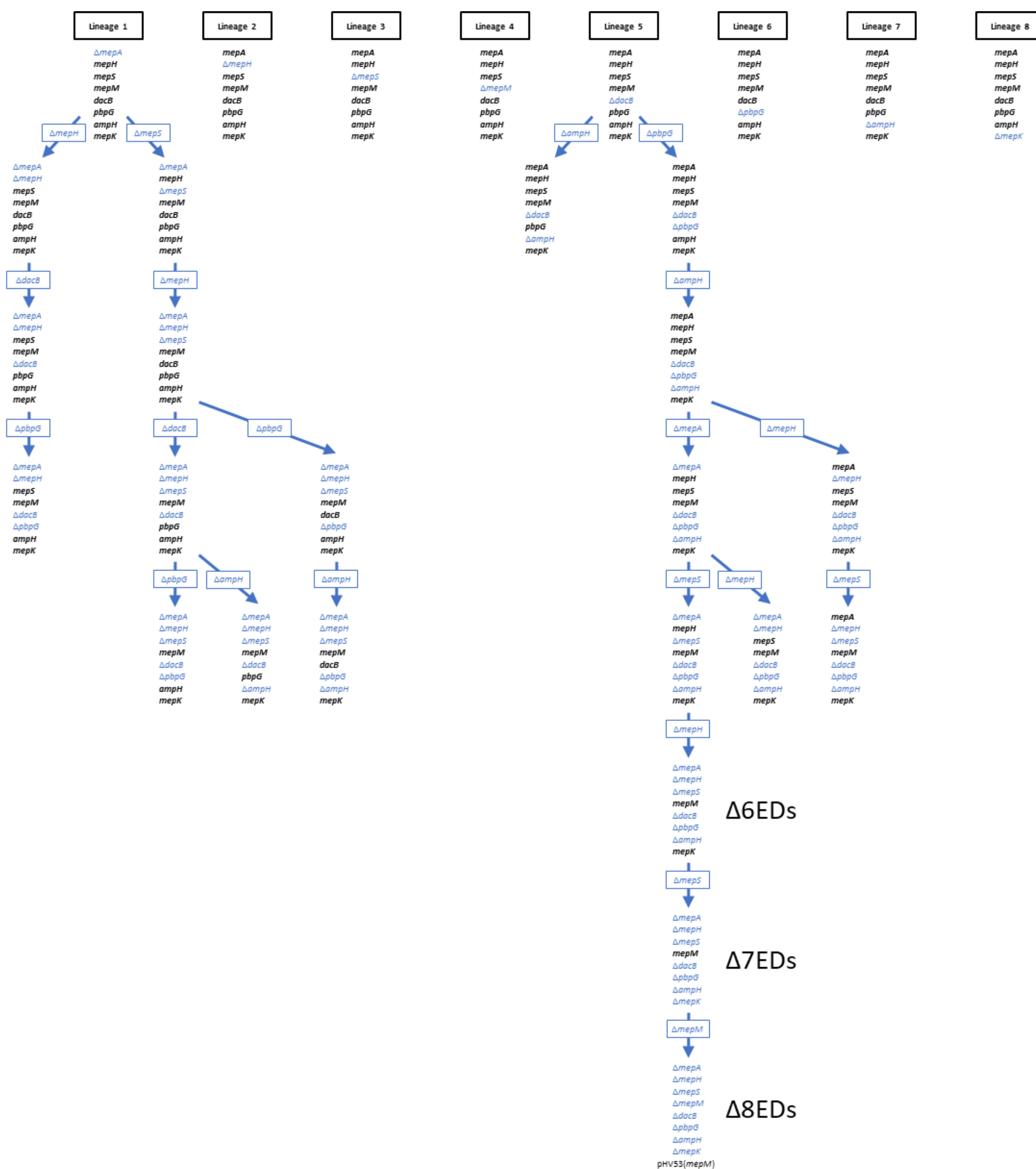

426

427 **Figure S4. Parallel and serial deletion of endopeptidase genes in *E. coli* BW25113 Δ*relA*.** Deletions
428 indicated in blue were introduced by the procedure of Datsenko and Wanner (Datsenko and Wanner,
429 2000). The remaining endopeptidase genes are indicated in black. The presence of all deletions was
430 verified by PCR at each steps. The genomes of the strains retaining *mepM* and *mepK* (Δ6EDs) or only *mepM*
431 (Δ7EDs) were re-sequenced and no compensatory mutation was detected.

432

433 **MepA and MepS compensate for the absence of MepK when *ycbB* is induced**

bioRxiv preprint doi: https://doi.org/10.1101/2021.02.12.430937; this version posted February 12, 2021. The copyright holder for this preprint (which was not certified by peer review) is the author/funder. All rights reserved. No reuse allowed without permission.

434 The basal production of the YcbB L,D-transpeptidase encoded by plasmid pKT2(*ycbB*) in the
435 absence of induction was found to be lethal in a derivative of BW25113 lacking *mepK* (above). To
436 investigate the possibility that MepK might be replaced by another endopeptidase, the *ycbB* gene
437 was cloned under the control of the P_{araBAD} promoter of vector pHV7 to obtain a lower level of
438 expression of the L,D-transpeptidase gene. The resulting plasmid, pHV63(*ycbB*) was successfully
439 introduced into the BW25113 Δ*mepK* strain indicating that the basal level of expression of *ycbB*
440 in the absence of induction was compatible with the absence of *mepK*. The disk diffusion assay
441 revealed a clear zone around the disk containing L-arabinose indicating that induction of *ycbB* in
442 the Δ*mepK* background prevented bacterial growth (Fig. 9A). Plasmids for expression of each of
443 the eight endopeptidases under the control of the P_{rhaBAD} promoter (above) were introduced in
444 this strain (Fig. 9B). Bacterial growth was observed in conditions of induction of *ycbB* by L-
445 arabinose and of genes encoding MepA and MepS by L-rhamnose. This result indicates that the
446 essential role of MepK for PG polymerization mediated by the YcbB L,D-transpeptidase was
447 bypassed by overproduction of MepA or MepS.
448

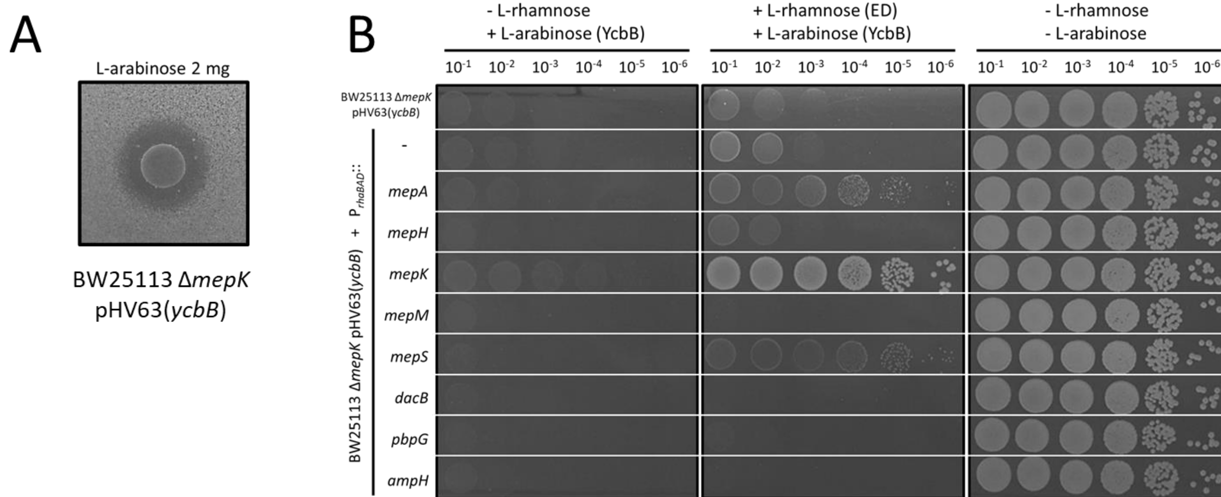

449

450 **Figure 9. Complementation of the *mepK* deletion by plasmids encoding L-rhamnose-inducible copies of**
451 **the eight endopeptidase genes.** (**A**) Induction of *ycbB* under the control of the P_{araBAD} promoter in
452 BW25113 Δ*mepK* pHV63(*ycbB*) was studied by the disk diffusion assay. The clear zone around the disk
453 containing L-arabinose indicates that production of YcbB inhibited growth. (**B**) Functional
454 complementation of the *mepK* deletion of BW25113 Δ*mepK* pHV63(*ycbB*) was performed with the pHV30
455 vector or recombinant plasmids encoding each of the eight endopeptidases under the control of the P_{rhaBAD}
456 promoter. Induction of *ycbB* and of endopeptidase (ED) genes was performed with 0.2% L-arabinose and

bioRxiv preprint doi: https://doi.org/10.1101/2021.02.12.430937; this version posted February 12, 2021. The copyright holder for this preprint (which was not certified by peer review) is the author/funder. All rights reserved. No reuse allowed without permission.

457 1% L-rhamnose, respectively. BHI agar plates contained chloramphenicol (20 µg/ml) to counter-select loss
458 of pHV63(*ycbB*).

459

460 **Complementation of the *mepK* deletion by catalytically inactivated endopeptidases**

461 Since overproduction of MepK, MepS, and MepA were found to complement the chromosomal
462 deletion of the *mepK* gene (above, Fig. 9) we focused on these three endopeptidases. Plasmids
463 encoding catalytically inactive MepK $H^{133}A$, MepS $C^{94}A$, and MepA $H^{113}A$ were used to determine
464 whether the endopeptidase activity of MepK, MepA, and MepS was required to compensate for
465 the chromosomal deletion of *mepK*. Overproduction of the endopeptidases was tested in the
466 Δ*mepK* background (single-deletion mutant retaining all chromosomal endopeptidase genes
467 except *mepK*) and in the Δ7EDs background (seven-deletion mutant retaining only *mepM*) (Fig.
468 10). Overproduction of MepK but not MepK $H^{133}A$ was essential for growth in both backgrounds
469 indicating that the catalytic activity of the endopeptidase was essential. Overproduction of MepS
470 restored growth in both backgrounds but complementation by MepS $C^{94}A$ was only observed in
471 the Δ*mepK* single-deletion background. Since the periplasmic protease Prc hydrolyzes MepS
472 (Singh et al., 2015) overproduction of MepS $C^{94}A$ may saturate the protease enabling sufficient
473 chromosomally-encoded MepS to escape hydrolysis and support growth. Likewise, saturation of
474 the Prc protease is likely to be responsible for the apparent complementation mediated by
475 overproduction of MepA and MepA $H^{113}A$ since overproduction of these enzymes restored
476 growth in the ΔmepK single-deletion background but not in the Δ7EDs background. Together
477 these results indicate that MepS is the only endopeptidase that can compensate for the absence
478 of MepK. This required overproduction of MepS. Alternatively, saturation of the Prc protease by
479 overproduction of MepA, MepA $H^{113}A$, or MepS $C^{94}A$ prevented hydrolysis of MepS produced at
480 a lower level from the native chromosomal *mepS* gene.

bioRxiv preprint doi: https://doi.org/10.1101/2021.02.12.430937; this version posted February 12, 2021. The copyright holder for this preprint (which was not certified by peer review) is the author/funder. All rights reserved. No reuse allowed without permission.

481 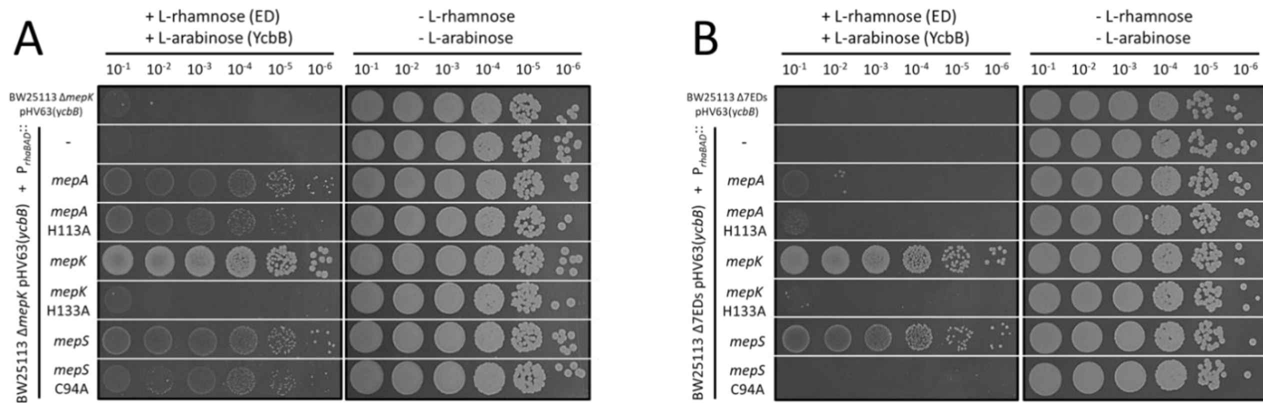

482 **Figure 10. Complementation of *mepK* deletion with catalytically inactivated endopeptidases.** (**A**)
483 Functional complementation of the *mepK* deletion of BW25113 Δ*mepK* pHV63(*ycbB*) was performed with
484 the pHV30 vector or recombinant plasmids encoding *mepA*, *mepK*, *mepS* or derivatives encoding
485 catalytically inactive endopeptidases under the control of the P_{rhaBAD} promoter. **(B)** The complementation
486 assay was repeated for BW25113 Δ7EDs pHV63(*ycbB*), which was obtained by deletion of all chromosomal
487 endopeptidase genes except *mepM.* Induction of *ycbB* and of endopeptidase (ED) genes was performed
488 with 0.2% L-arabinose and 1% L-rhamnose, respectively. BHI agar plates contained chloramphenicol (20
489 µg/ml) to counte-select loss of pHV63(*ycbB*).

490

491 **Minimal complement of endopeptidases required for growth in the presence of β-lactams in**
492 **the context of the exclusive formation of 3→3 cross-links by the YcbB L,D-transpeptidase**

493 As previously described (Hugonnet et al., 2016), induction of *relA'* led to mecillinam resistance in
494 BW25113(*ycbB*, *relA'*) whereas induction of both *ycbB* and *relA'* was required for ampicillin and
495 ceftriaxone resistance (Table 1 and supplementary Fig. S5). Strain BW25113(*ycbB*, *relA'*) Δ6EDs
496 was also resistant to the three β-lactams upon induction of *ycbB* and *relA'* indicating that 6 of the
497 8 endopeptidase genes were dispensable for expression of β-lactam resistance. In contrast to
498 BW25113(*ycbB*, *relA'*), the Δ6EDs derivative was resistant to ampicillin and ceftriaxone in the
499 absence of induction of *ycbB* by IPTG. The basal level of *ycbB* expression in the absence of
500 induction was required for resistance since susceptibility to ampicillin and ceftriaxone was
501 observed in the absence of pKT2(*ycbB*). These observations indicate that deletion of 6 of the 8
502 endopeptidase genes was associated with a decrease in the level of expression of *ycbB* required
503 for β-lactam resistance. In combination with the analysis based on single-gene deletions (Fig. 2B),
504 these results show that MepM and MepK are necessary and sufficient for bacterial growth in
505 conditions in which YcbB is the only functional transpeptidase.

bioRxiv preprint doi: https://doi.org/10.1101/2021.02.12.430937; this version posted February 12, 2021. The copyright holder for this preprint (which was not certified by peer review) is the author/funder. All rights reserved. No reuse allowed without permission.

506

Table 1. YcbB-mediated β-lactam resistance in BW25113 derivatives harboring all endopeptidase genes or only *mepM* and *mepK* (Δ6ED)

Host			Inhibition zones (mm)[a]		
	Plasmid	Inducer[b]	Mec	Amp	Cro
BW25113 Δ*relA*					
	pKT2(*ycbB*) pKT8(*relA′*)	None	24	22	38
		IPTG (*ycbB*)	28	24	39
		Ara (*relA′*)	< 8	24	39
		IPTG + Ara	< 8	< 8	18
BW25113 Δ*relA* Δ6EDs					
	pKT2(*ycbB*) pKT8(*relA′*)	None	17	27	41
		IPTG (*ycbB*)	17	28	43
		Ara (*relA′*)	< 8	< 8	22
		IPTG + Ara	< 8	< 8	19
BW25113 Δ*relA* Δ6EDs					
	pKT8(*relA′*)	None	17	27	41
		Ara (*relA′*)	< 8	27	41

507 [a] The diameter of inhibition zones was determined by the disk diffusion assay around
508 disks containing 10 µg mecillinam (Mec), 10 µg ampicillin (Amp), or 30 µg ceftriaxone
509 (Cro). Examples of the original results are presented in supplementary Fig. S5.
510 [b] The *ycbB* and *relA′* genes carried by plasmid pKT2 and pKT8 were induced with 40
511 µM IPTG and 1% L-arabinose (Ara), respectively.

bioRxiv preprint doi: https://doi.org/10.1101/2021.02.12.430937; this version posted February 12, 2021. The copyright holder for this preprint (which was not certified by peer review) is the author/funder. All rights reserved. No reuse allowed without permission.

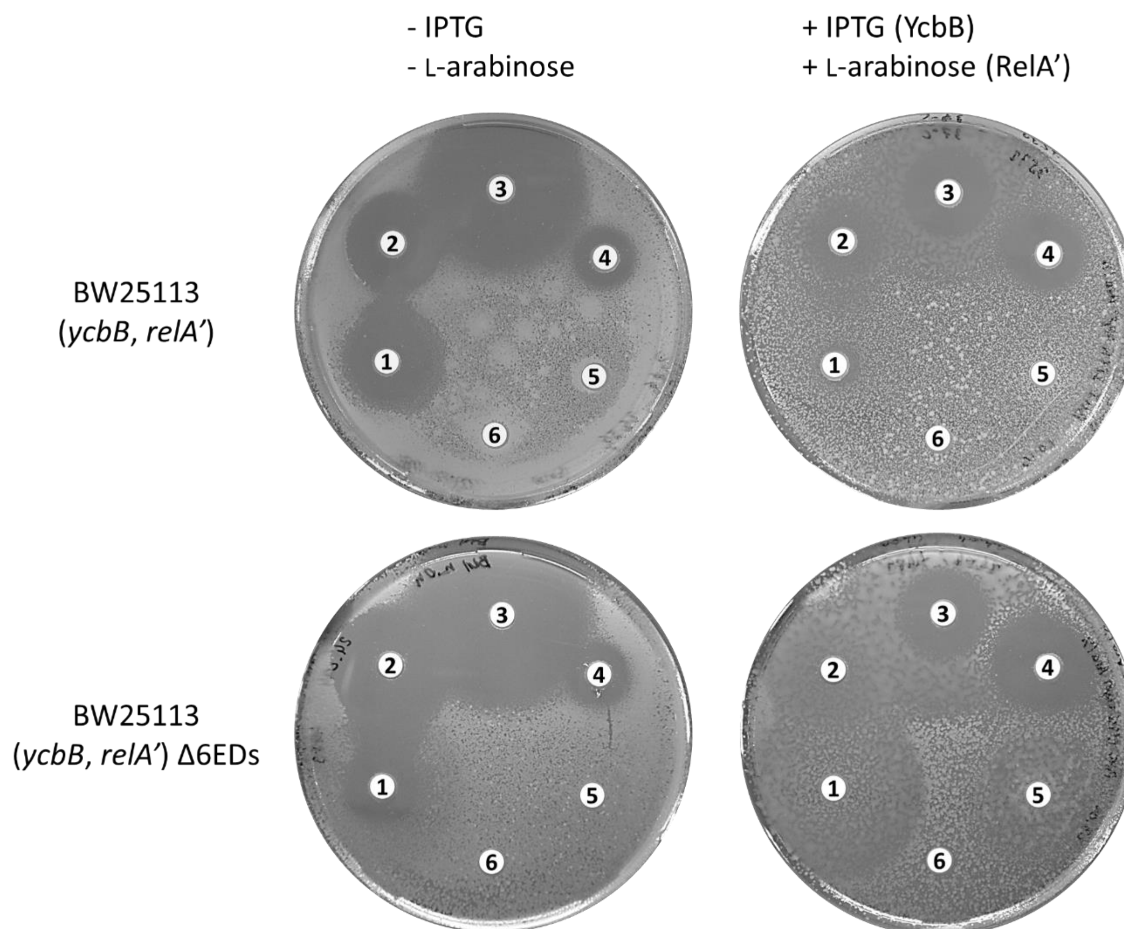

512

513 **Figure S5. Antibiotic susceptibility testing by the disk diffusion assay.** Disks contained 10 µg mecillinam
514 (1), 10 µg ampicillin (2), 30 µg ceftriaxone (3), 30 µg tetracycline (4), 30 µg chloramphenicol (5), and 30 µg
515 kanamycin (6). Plasmids pKT2(*ycbB*) and pKT8(*relA'*) confer resistance to tetracycline and
516 chloramphenicol, respectively. Kanamycin resistance is mediated by the Km^R cassette inserted in place of
517 *relA*. Induction of *ycbB* and *relA'* was performed with 40 µM IPTG and 1% L-arabinose.

518

519 **Mutations impairing the lytic transglycosylase activity of Slt70 favors YcbB-mediated PG**
520 **synthesis**

521 Although BW25113(*ycbB*, *relA'*) displays high β-lactam resistance on BHI agar supplemented with
522 IPTG and L-arabinose, the strain was found to remain susceptible to β-lactams in BHI broth
523 supplemented with the same inducers. Mutations leading to expression of β-lactam resistance in
524 liquid medium were sought by selecting mutants derived from *E. coli* BW25113 M1 (Hugonnet et
525 al., 2016). The latter strain overexpresses *ycbB* carried by plasmid pJEH12(*ycbB*) in response to
526 induction by IPTG and overproduces the (p)ppGpp alarmone due to impaired expression of the

bioRxiv preprint doi: https://doi.org/10.1101/2021.02.12.430937; this version posted February 12, 2021. The copyright holder for this preprint (which was not certified by peer review) is the author/funder. All rights reserved. No reuse allowed without permission.

527 isoleucine tRNA synthetase gene *ileS* (Hugonnet et al., 2016). Derivatives of BW25113 M1 were
528 selected in BHI broth containing 16 µg/ml ampicillin and 50 µM IPTG. Four independent mutants
529 derived from BW25113 M1 (M1.1 to M1.4) were isolated and shown to grow in liquid medium
530 supplemented with ampicillin and IPTG (Fig. 11A). Whole genome sequencing revealed single
531 mutations all located in the *sltY* gene encoding the Slt70 lytic transglycosylase (Table 2). One of
532 the mutants (M1.3) most probably harbored a null allele of *sltY* since a 7-bp deletion introduced
533 a frame-shift at the 9th codon of the gene. To confirm this conclusion, the *sltY* gene was deleted
534 from the chromosome of BW25113(*ycbB*, *relA'*) strain. The resulting strain, BW25113(*ycbB*, *relA'*)
535 Δ*sltY*, was also resistant to ampicillin in liquid medium. Growth of BW25113(*ycbB*, *relA'*) Δ*sltY* in
536 the presence of ampicillin in liquid medium required the presence of IPTG and L-arabinose
537 indicating that overproduction of both the YcbB L,D-transpeptidase and of RelA' remained
538 essential for β-lactam resistance. Comparison of the resistance phenotype of BW25113(*ycbB*,
539 *relA'*) and its Δ*sltY* derivative on BHI agar revealed that overproduction of YcbB upon induction
540 by IPTG was dispensable for β-lactam resistance in the absence of Slt70 (Fig 11B). However,
541 expression of β-lactam resistance on BHI agar remained dependent upon induction of RelA' by L-
542 arabinose and upon the presence of pKT2(*ycbB*). These results indicate that loss of Slt70 was
543 essential for expression of YcbB-mediated β-lactam resistance in liquid medium and reduced the
544 level of production of the YcbB L,D-transpeptidase required for expression of resistance on solid
545 medium. This observation suggests that accumulation of uncross-linked glycan chains in the
546 absence of Slt70 may improve the capacity of YcbB to catalyze PG cross-linking accounting for the
547 lower level of expression of *ycbB* required for resistance.

548
Table 2. Mutations detected in the *sltY* gene of mutants BW25113 M1.1 to M1.4
549

Mutant	Position	Mutation	Impact[a]
M1.1	4,621,672	C→T	Gln^{375}stop
M1.2	4,622,297	Duplication of AGG CAGGG→CAGGAGGG	Insertion of Gly position 584 (codon GGN)
M1.3	4,620,572	7-bp deletion CCTGGCGGC→CC	Trp^{9}frameshift
M1.4	4,621,507	C→T	Arg^{320}stop

550

551 [a] Slt70 comprises 645 amino acid residues.
552

bioRxiv preprint doi: https://doi.org/10.1101/2021.02.12.430937; this version posted February 12, 2021. The copyright holder for this preprint (which was not certified by peer review) is the author/funder. All rights reserved. No reuse allowed without permission.

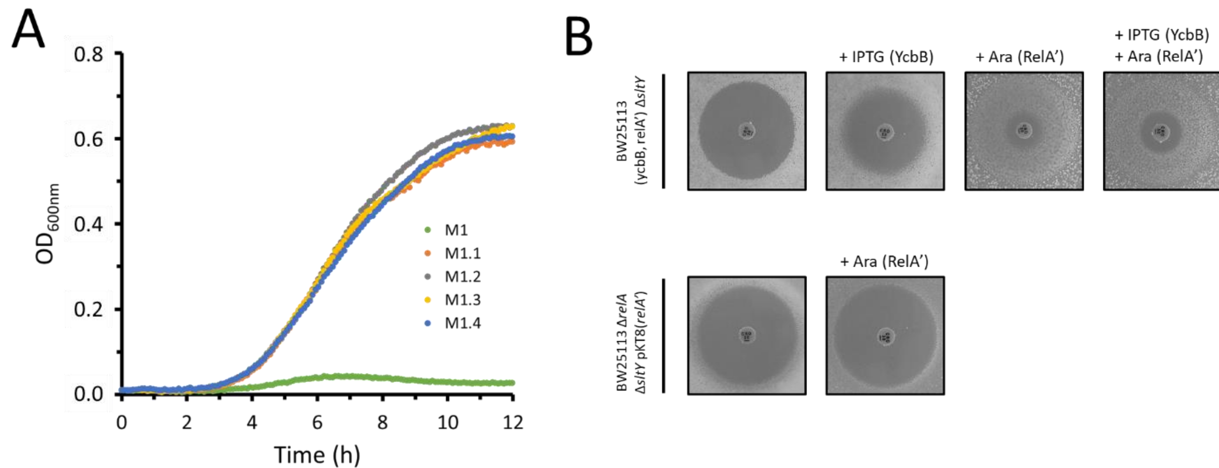

553

554 **Figure 11. Growth phenotype of *sltY* mutants.** (**A**) Growth curves of parental strain M1 and mutants M1.1
555 to M1.4 selected for expression of ampicillin resistance in BHI broth. The growth medium contained 50
556 µM IPTG and 16 µg/ml ampicillin. (**B**) Ceftriaxone-resistance depends upon *ycbB* and *relA'* expression. The
557 disk diffusion assay was performed with BW25113 Δ*relA* Δ*sltY* harboring pKT2(*ycbB*) and pKT8(*relA'*) or
558 pKT8(*relA'*) only. Induction was performed with 40 µM IPTG and 1% L-arabinose for *ycbB* and *relA'*,
559 respectively. Disks were loaded with 30 µg of ceftriaxone.

560

561 **DISCUSSION**

562 **Endopeptidases are essential for expansion of sacculi**

563 PG polymerization requires a combination of synthetases, the transpeptidases and the
564 glycosyltransferases, in addition to hydrolases that fulfill two essential roles. Since PG is a net-like
565 macromolecule completely surrounding the bacterial cell it is beyond any required experimental
566 demonstration that insertion of new disaccharide-peptide subunits into the growing cell wall
567 requires cleavage of covalent bonds (Höltje and Heidrich, 2001; Vollmer, 2012). The stress-
568 bearing PG being present during the entire cell cycle, it is also obvious that PG hydrolases are
569 required to split daughter cells following completion of septum synthesis (Heidrich et al., 2002).
570 A portion of these hydrolases generate PG fragments that are imported into the cell and recycled,
571 a complex pathway that is not essential for growth in laboratory conditions but bears important
572 roles in (i) minimizing energy costs, (ii) sensing the appropriate balance between synthetic and
573 hydrolytic activities, which may be altered by β-lactam antibiotics and other toxic agents, and (iii)
574 avoiding the release of proinflammatory molecules recognized by the host immune system
575 (Bastos et al., 2020; Johnson et al., 2013). PG hydrolases specifically acting on each of the ten

bioRxiv preprint doi: https://doi.org/10.1101/2021.02.12.430937; this version posted February 12, 2021. The copyright holder for this preprint (which was not certified by peer review) is the author/funder. All rights reserved. No reuse allowed without permission.

576 amide, ether, and glycosidic bonds present in the PG polymer have been described and most
577 cleavage specificities involve multiple enzymes (supplementary Fig. S6A). Enzymes of different
578 specificities can at least in part compensate for each other, *e.g*. lytic glycosyltransferases and
579 amidases both contribute to the separation of daughter cells (Heidrich et al., 2002; van
580 Heijenoort, 2011). In this study, we show that endopeptidases are specifically required for
581 bacterial growth not only in the context of the formation of 4→3 cross-links by PBPs but also in
582 the context of the formation of 3→3 cross-links by YcbB (Table 3). We also identify for the first
583 time the minimum sets of endopeptidases for each mode of PG cross-linking, namely MepM for
584 4→3 cross-links and MepM plus MepK for 3→3 cross-links. Endopeptidase overproduction
585 resulting from expression of the genes under the control of heterologous promoters revealed
586 potential functional redundancies in the endopeptidase families. In particular, overproduction of
587 MepH, MepS, or PBP7 compensated for the absence of MepM in the context of a 4→3 cross-
588 linked PG. Overproduction of MepS compensated for the absence of MepM or MepK for growth
589 with a 3→3 cross-linked PG. Overproduction of MepM prevented growth probably due to
590 unbalanced synthesis and hydrolysis of PG cross-links (observed for both 4→3 and 3→3 cross-
591 linked PG). Production of catalytically inactive endopeptidases suggested that MepA and MepS
592 are negatively regulated by Prc-mediated proteolysis, as previously established for MepS (Lai et
593 al., 2017; Singh et al., 2015).

594

595 **Specificity of purified endopeptidases for 4→3 and 3→3 cross-links**

596 The cleavage specificity of the endopeptidases was determined by mass spectrometry (Fig. 5, 7,
597 and S2). Endopeptidases of the PBP family were specific to 4→3 cross-links. Endopeptidases
598 belonging to other families cleaved both 4→3 and 3→3 cross-links with similar efficacies (MepM,
599 MepS, MepA) or with a preference for 4→3 (MepH) or 3→3 (MepK) cross-links (Fig. 5 and 7)
600 (Chodisetti and Reddy, 2019; Engel et al., 1992). This is unexpected since 4→3 and 3→3 cross-
601 links contain amide bonds connecting two R stereo centers (D-Ala^{4}→DAP^{3}) or an S to an R stereo
602 center (DAP^{3}→DAP^{3}), respectively (supplementary Fig. S6A). This could imply that
603 endopeptidases of the Mep families mainly interact with the acceptor stems of cross-linked
604 muropeptides, which are the same for both types of cross-links, whereas endopeptidases of the

bioRxiv preprint doi: https://doi.org/10.1101/2021.02.12.430937; this version posted February 12, 2021. The copyright holder for this preprint (which was not certified by peer review) is the author/funder. All rights reserved. No reuse allowed without permission.

605 PBP family interact with a donor tetrapeptide stem only present in 4→3 cross-linked
606 muropeptides (supplementary Fig. S6B).

607

608 **Integration of endopeptidases into the global regulation of 4→3 and 3→3 PG cross-linking**

609 D,D-carboxypeptidases, which cleave off the terminal residue (D-Ala^5) of pentapeptide stems, are
610 thought to negatively control the transpeptidase activity of PBPs since these enzymes require a
611 pentapeptide donor (Fig. 1). A less studied impact of D,D-carboxypeptidases is the formation of
612 the essential tetrapeptide donor substrate of the LDTs, except for two publications reporting that
613 PBP5 and PBP6a are essential for YcbB-mediated β-lactam resistance and for rescue of a defect
614 in lipopolysaccharide synthesis, respectively (Hugonnet et al., 2016; Morè et al., 2019). Thus, D,D-
615 carboxypeptidases have crucial roles in controlling the relative contributions of transpeptidases
616 of the D,D and L,D specificities to PG cross-linking by both decreasing access of PBPs to
617 pentapeptide stems and increasing access of LDTs to tetrapeptide stems.

618 Endopeptidases participate in the metabolism of PG cross-links in several ways. MepH and
619 MepS display L,D-carboxypeptidase activity leaving tripeptides as the main (> 80%) end product
620 of *in vitro* PG hydrolysis (Fig. 7). This activity may negatively control the L,D-transpeptidase activity
621 of YcbB by hydrolysis of D-Ala^4 thereby preventing access to its tetrapeptide donor. In addition,
622 hydrolysis of 4→3 cross-linked Tetra→Tetra and Tetra→Tri dimers by the endopeptidases
623 generates free tetrapeptide stems (Fig. 5 and 7). These tetrapeptide stems can be used as donor
624 by YcbB for formation of 3→3 cross-links, as demonstrated for the LDTs of *Mycobacterium*
625 *smegmatis* (Baranowski et al., 2018). In contrast, the D,D-transpeptidase activity of PBPs
626 exclusively relies on *de novo* synthesis and translocation of pentapeptide-containing precursors
627 since the D-Ala^5 residue of pentapeptide stems is rapidly cleaved off by D,D-carboxypeptidases if
628 they are not used for formation of 4→3 cross-links. Thus, YcbB is expected to function as a rescue
629 enzyme to restore cross-linking in regions of the PG that are compromised by 4→3 or 3→3
630 endopeptidases. This mechanism was proposed for PG reparation following disassembly of the
631 lipopolysaccharide export machinery that crosses the PG layer (Morè et al., 2019). The combined
632 activities of endopeptidases cleaving 4→3 cross-links and of L,D-transpeptidases could contribute

bioRxiv preprint doi: https://doi.org/10.1101/2021.02.12.430937; this version posted February 12, 2021. The copyright holder for this preprint (which was not certified by peer review) is the author/funder. All rights reserved. No reuse allowed without permission.

633 to the enrichment in 3→3 cross-links in stationary phase cultures (Pisabarro et al., 1985). In turn,
634 this enrichment may protect cells from hydrolases active on 4→3 cross-linked PG. Previous
635 analyses proposed that two L,D-transpeptidases may contribute to the enrichment of PG in 3→3
636 cross-links, namely YcbB (LdtD), induced by the cell envelope Cpx stress system, and YnhG (LdtE),
637 expressed under the control of sigma S and induced in stationary phase (Delhaye et al., 2016;
638 Weber et al., 2005).

639

640 **Participation of YcbB to PG polymerization complexes**

641 PG polymerization is generally thought to be performed by two multiprotein complexes involved
642 in the expansion of the lateral cell wall (elongasome) and in the formation of the septum
643 (divisome) (Pazos et al., 2017). Replacement of the D,D-transpeptidase activity of all PBPs by the
644 L,D-transpeptidase activity of YcbB raises several questions regarding the identity of the partners
645 of YcbB for the assembly of lateral wall and septum PG, and whether YcbB physically replaces
646 PBPs in the PG polymerization complexes. Our data support a model in which YcbB functions with
647 two different sets of partners for lateral wall and septum PG assembly as follows.

648 For the assembly of lateral wall PG, inactivation of the transpeptidase domain of PBP2 by β-
649 lactams leads to uncoupling of the transglycosylation and transpeptidation reactions, the former
650 being most probably catalyzed by RodA (Cho et al., 2014; Uehara and Park, 2008). Uncross-linked
651 glycan chains accumulate in the periplasm and are eventually cleaved by the Slt70 lytic
652 transglycosylase and recycled. According to the model presented in Fig. 12, and in agreement
653 with a previous study (Cho et al., 2014), the reactions catalyzed by Slt70 and YcbB occur in
654 competition implying that YcbB-mediated cross-linking is not coupled to glycan chain
655 polymerization by RodA. This also implies that YcbB could function in the PG layer in combination
656 with the MepM endopeptidase known to participate in cell elongation (Banzhaf et al., 2020; Singh
657 et al., 2012; Truong et al., 2020; Uehara et al., 2009). In agreement with this model, impaired
658 Slt70 activity had a positive impact on β-lactam resistance mediated by YcbB. This was established
659 both by the selection of mutations enabling expression of β-lactam resistance in liquid medium,

bioRxiv preprint doi: https://doi.org/10.1101/2021.02.12.430937; this version posted February 12, 2021. The copyright holder for this preprint (which was not certified by peer review) is the author/funder. All rights reserved. No reuse allowed without permission.

660 which mapped in the *sltY* gene encoding Slt70 (Table 2) and by the deletion of *sltY*, which lowered
661 the level of *ycbB* expression required for resistance (Fig. 11).

662 For the assembly of septum PG, YcbB was proposed to cooperate with the glycosyltransferase
663 activity of Class A PBP1b (Caveney et al., 2019; Hugonnet et al., 2016). In support of this
664 hypothesis, microscale thermophoresis experiment revealed that purified YcbB interacts with
665 PBP1b and PBP5 (D,D-carboxypeptidase). Furthermore, the glycosyltransferase activity of PBP1b
666 is essential for YcbB-mediated β-lactam resistance whereas the combined deletion of class A
667 PBP1a and PBP1c had no impact. We cannot rule out the possibility that the glycosyltransferase
668 activity of FtsW also contributes to septum PG polymerization in the presence of β-lactams but
669 this would require that the inactivation of PBP3 by β-lactams lead to the uncoupling of glycan
670 chain polymerization and PG cross-linking, as proposed for the RodA-PBP2 complex (see above).
671 This is not supported by the analyses of PG recycling in conditions of selective inhibition of PBP3
672 by aztreonam (Uehara and Park, 2008). The endopeptidases involved in septum formation have
673 not been identified, except for a contribution of PBP4, which has an effect on the timing of
674 septation (Verheul et al., 2020). MepK is a candidate for this function in 3→3 cross-linked PG
675 although this is currently not supported by any experimental evidence and it remains to be seen
676 if endopeptidases are needed for septum PG synthesis.
677

bioRxiv preprint doi: https://doi.org/10.1101/2021.02.12.430937; this version posted February 12, 2021. The copyright holder for this preprint (which was not certified by peer review) is the author/funder. All rights reserved. No reuse allowed without permission.

678

Table 3. Characteristics of the endopeptidases

Endopeptidase	*In vitro* hydrolysis of 4→3 and 3→3 cross-links[c]	Role in the context of the two modes of cross-linking (revealed by endopeptidase overproduction[f])	
		4→3 cross-links	**3→3 cross-links**
Acyl-serine transferase			
PBP4[a]	4→3	Not essential (None)	Not essential (None)
PBP7[a]	4→3	Not essential (Compensates for the absence of MepM)	Not essential (None)
AmpH[b]	4→3[d]	Not essential (None)	Not essential (None)
NlpC/P60 peptidase			
MepH[a]	4→3 > 3→3 L,D-carboxypeptidase	Not essential (Compensates for the absence of MepM)	Not essential (None)
MepS[a]	4→3 = 3→3 L,D-carboxypeptidase	Not essential (Compensates for the absence of MepM)	Not essential (Compensates for the absence of MepM or MepK)[e]
Lysostaphin/M23 peptidase			
MepM[a]	4→3 = 3→3	Sufficient (Prevents growth)	Essential (Prevents growth)
LAS metallopeptidase			
MepA[b]	4→3 = 3→3	Not essential (None)	Not essential (None)
M15 peptidase			
MepK[b]	4→3 < 3→3	Not essential (None)	Essential (None)

679 [a] Characterized in this study.
680 [b] Data from the literature (Chodisetti and Reddy, 2019; Engel et al., 1992; Gonzalez-Leiza et al., 2011).
681 [c] MepM, MepS, and MepA cleaved 4→3 and 3→3 cross-links with similar efficacies (4→3 = 3→3). MepH
682 and MepK displayed a preference for 4→3 cross-links (4→3 > 3→3) or for 3→3 cross-links (4→3 < 3→3),
683 respectively. L,D-carboxypeptidase, hydrolysis of the DAP[3]-D-Ala[4] amide bond of tetrapeptide stems.
684 [d] Hydrolysis of 3→3 cross-links was not tested.
685 [e] Replacement of both MepM and MepK by MepS was not tested.
686 [f] None, no phenotype associated with endopeptidase overproduction.

bioRxiv preprint doi: https://doi.org/10.1101/2021.02.12.430937; this version posted February 12, 2021. The copyright holder for this preprint (which was not certified by peer review) is the author/funder. All rights reserved. No reuse allowed without permission.

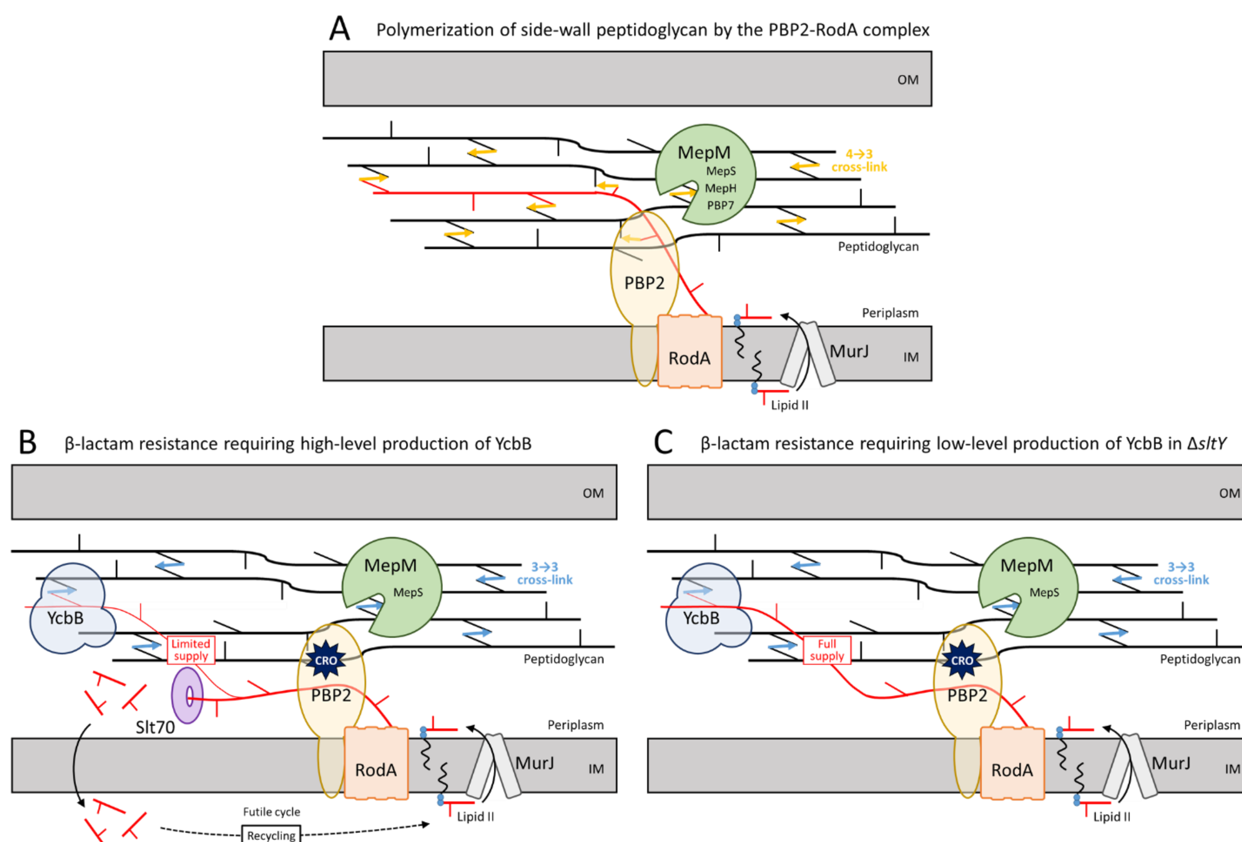

687

688 **Figure 12. Proposed model for polymerization of side wall PG by transpeptidases of the D,D- or L,D-**
689 **specificity.** (**A**) In wild-type cells, the disaccharide pentapeptide subunit linked to the undecaprenyl lipid
690 transporter (Lipid II) is translocated to the outer leaflet of the cytoplasmic membrane by MurJ and
691 polymerized by the glycosyltransferase and D,D-transpeptidase activities of the PBP2-RodA complex.
692 MepM is essential and sufficient for insertion of new material in the PG net, although this endopeptidase
693 can be replaced by overproduction of MepH, MepS, or PBP7. (**B**) Inhibition of PBP2 by β-lactams leads to
694 the accumulation of uncross-linked glycan chains that are cleaved by the Slt70 lytic transglycosylase. This
695 limits the supply of glycan chains for cross-linking by the YcbB L,D-transpeptidase. Under this condition,
696 MepM or overproduction of MepS is required for insertion of new glycan strands. (**C**) Deletion of the *sltY*
697 gene encoding lytic transglycosylase Slt70 prevents digestion of uncross-linked glycan chains leading to a
698 full supply of neo-synthesized glycan chains to YcbB and improved expression of β-lactam resistance. IM,
699 inner membrane; OM, outer membrane; CRO, ceftriaxone.
700

bioRxiv preprint doi: https://doi.org/10.1101/2021.02.12.430937; this version posted February 12, 2021. The copyright holder for this preprint (which was not certified by peer review) is the author/funder. All rights reserved. No reuse allowed without permission.

A

1a Muramidase
1b Lytic transglycosylase
2 Glucosaminidase
3 D,D-carboxypeptidase
4 L,D-carboxypeptidase
5 Etherase
6 Amidase
7 L-Ala-D-iGlu endopeptidase
8 D-iGlu-DAP endopeptidase
9 DAP-D-Ala endopeptidase
10 Endopeptidase 4→3
11 Endopeptidase 3→3

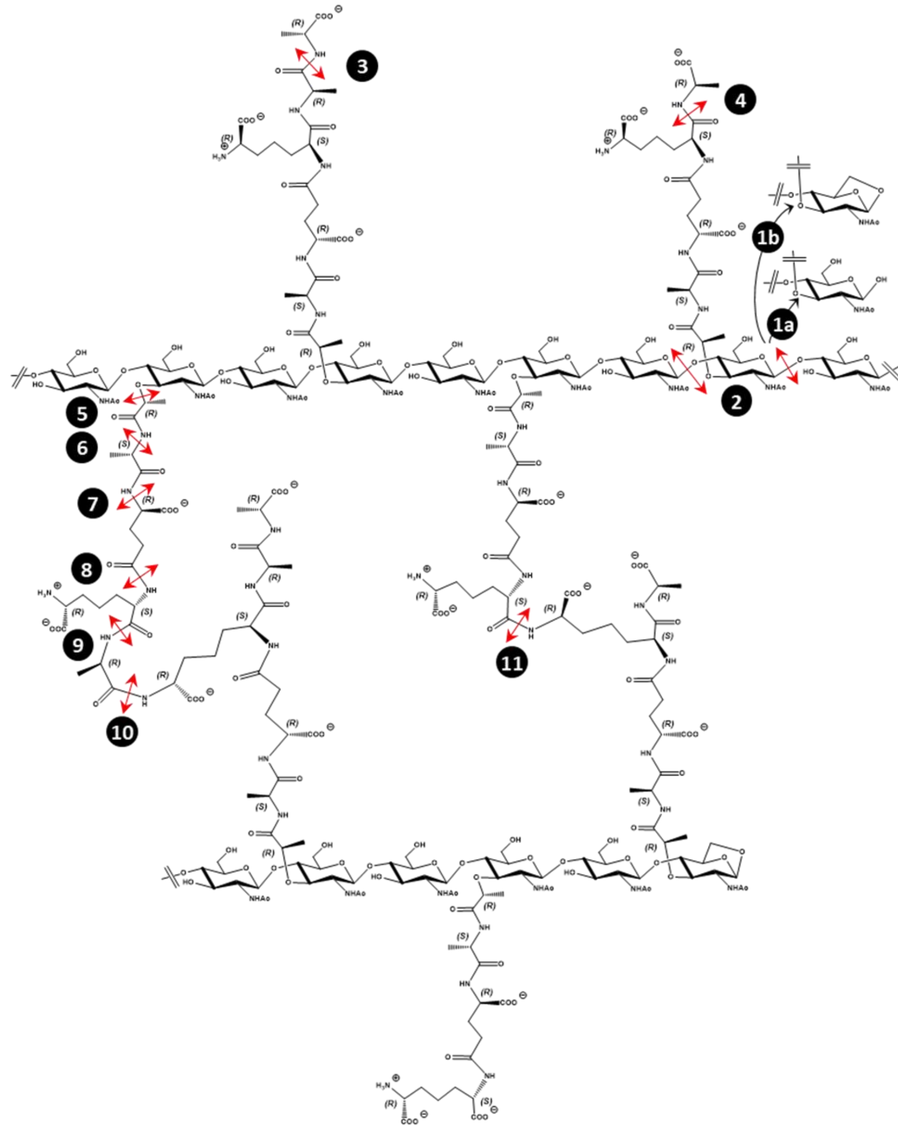

B

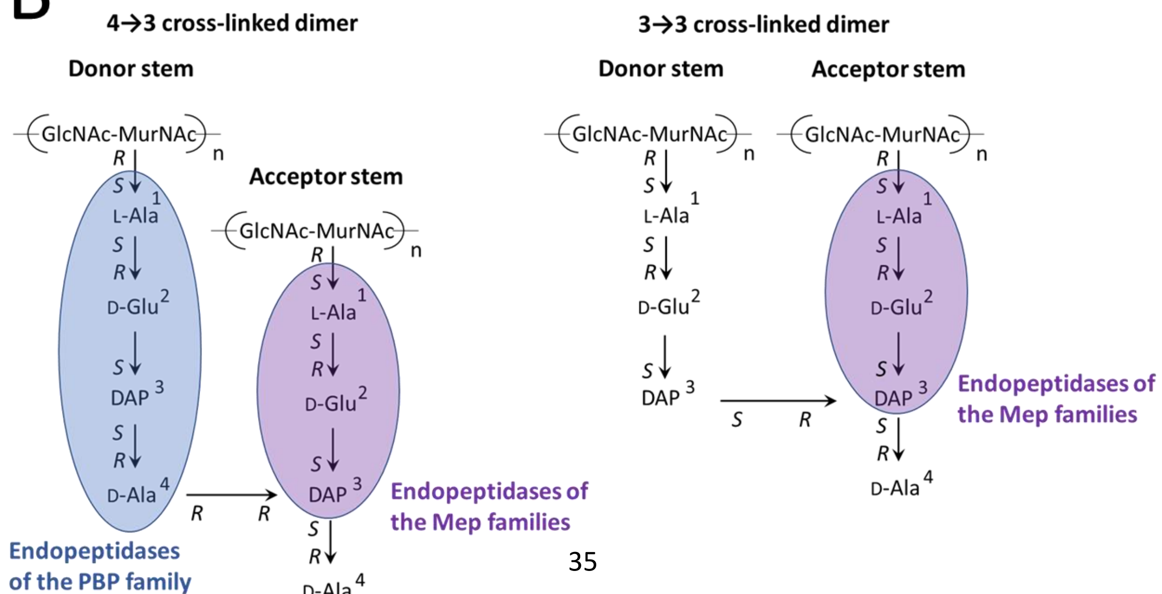

701

bioRxiv preprint doi: https://doi.org/10.1101/2021.02.12.430937; this version posted February 12, 2021. The copyright holder for this preprint (which was not certified by peer review) is the author/funder. All rights reserved. No reuse allowed without permission.

702 **Figure S6. Specificity of PG hydrolases.** (**A**) Highlight of enzyme stereospecificity. The commonly used
703 endopeptidase designation was employed in the entire manuscript to refer to the cleavage of internal
704 bonds although certain enzymes do not cleave peptide bonds connecting the α amino and carboxyl groups
705 of two consecutive amino acids and should have been more precisely referred to as amidases. (**B**).
706 Recognition of the donor and acceptor stems of dimers by PBP and Mep endopeptidases accounting for
707 the 4→3 *versus* 4→3 plus 3→3 specificities. According to this model, endopeptidases of the Mep families
708 cleave both 4→3 plus 3→3 cross-links since they interact with the tripeptide portion of the acceptor stem,
709 which is present in both types of dimers. In contrast, endopeptidases of the PBP families specifically
710 interact with the tetrapeptide donor stem of 4→3 cross-linked dimers.
711

712 **MATERIALS AND METHODS**

713 **Strains, plasmids, and growth conditions.** All strains were derived from *E. coli* BW25113 (Baba et
714 al., 2006). The origin and characteristics of plasmids are listed in Supplementary Table S1. Bacteria
715 were grown in brain heart infusion (BHI; Difco) broth or agar at 37 °C unless otherwise specified.
716 Liquid cultures were performed with aeration (180 rpm). The growth media were systemically
717 supplemented with drugs to counter-select plasmid loss (Supplementary Table S1). The same
718 drugs at the same concentrations were used to select transformants. Kanamycin at 50 µg/ml was
719 used for the Km^R cassette. Induction of the *lacZYA*, *araBAD*, and *rhaBAD* promoters was
720 performed with isopropyl β-D-1-thiogalactopyranoside (IPTG, 40 or 50 µM), L-arabinose (0.2 or
721 1%), and L-rhamnose (0.2 or 1%), respectively. Plasmids constructed in this study were obtained
722 by using NEBuilder HiFi DNA assembly (New England Biolabs) method, unless otherwise specified.
723 Growth curves were obtained in a 96-well plate using an Infinite 200 PRO microplate reader
724 (TECAN). Briefly, bacteria were grown to the late exponential phase, *i.e.* to an optical density at
725 600 nm (OD_{600}) greater than 1.0 (*ca*. 6 h at 37 °C under agitation). The OD_{600} was adjusted to 1.0
726 and 5 µl were inoculated in 195 µl of BHI broth supplemented with drugs and inducers, as
727 specified in the legends to figures. Growth was monitored at 600 nm every 5 min for 12 h at 37
728 °C with vigorous shaking.
729

730 **Construction of *E. coli* strains carrying gene deletions.** The Keio collection comprises 3,985
731 mutants obtained by replacement of non-essential genes by a kanamycin resistance (Km^R)
732 cassette (Baba et al., 2006). P1 transduction of the Km^R cassette from selected mutants was used
733 to introduce deletions of specific genes involved in PG synthesis (Datsenko and Wanner, 2000).
734 For multiple gene deletions, the Km^R cassette was removed by the FLT recombinase encoded by

bioRxiv preprint doi: https://doi.org/10.1101/2021.02.12.430937; this version posted February 12, 2021. The copyright holder for this preprint (which was not certified by peer review) is the author/funder. All rights reserved. No reuse allowed without permission.

735 plasmid pCP20. The presence of the expected deletions was confirmed by PCR amplification at
736 each deletion step. Supplementary Fig. S4 shows lineages that have been obtained by parallel
737 serial deletions.

738 To study the 3→3 mode of cross-linking, plasmid pKT2(*ycbB*) and pKT8(*relA'*) were introduced
739 into the derivatives of *E. coli* BW25113 Δ*relA* obtained by deletion of various combinations of
740 endopeptidase genes. For the sake of simplicity, the latter strains were referred to as
741 BW25113(*ycbB*, *relA'*) derivatives even though gene deletions preceded the introduction of
742 pKT2(*ycbB*) and pKT8(*relA'*).

743

744 **Construction of *E. coli* BW25113 Δ*relA* Δ8EDs.** The plasmid pHV53(P_{rhaBAD}-TIS2-*mepM*) was
745 introduced into BW25113 Δ*relA* Δ7EDs harboring *mepM* as the only chromosomal
746 endopeptidase-encoding gene. The *mepM* deletion was introduced into BW25113 Δ*relA* Δ7EDs
747 pHV53(P_{rhaBAD}-TIS2-*mepM*) in the presence of 0.2% L-rhamnose by P1 transduction as described
748 above. Growth of the resulting BW25113 Δ*relA* Δ8EDs pHV53(P_{rhaBAD}-TIS2-*mepM*) strain was
749 dependent on the induction of the plasmid copy of *mepM* mediated by L-rhamnose.

750

751 **Mutant selection and whole-genome sequencing.** *E. coli* BW25113 M1 was streaked for isolated
752 colonies on agar plates containing 10 µg/ml tetracycline to counter-select loss of plasmid
753 pJEH12(*ycbB*). The selection procedure was independently carried out starting with four
754 independent colonies. Briefly, 5 ml of BHI broth supplemented with 10 µg/ml tetracycline and 50
755 µM IPTG were inoculated with a colony. Bacteria were grown overnight with shaking (180 rpm).
756 A fraction of 1 ml of the culture was inoculated in 250 ml of BHI broth supplemented with 16
757 µg/ml ampicillin and 50 µM IPTG. Bacteria were grown overnight with shaking and streaked on
758 BHI agar containing 16 µg/ml ampicillin and 50 µM IPTG. A colony was inoculated in 250 ml of BHI
759 broth supplemented with 16 µg/ml ampicillin and 50 µM IPTG. Bacteria were grown overnight
760 with shaking and streaked on BHI agar containing 16 µg/ml ampicillin and 50 µM IPTG. Five ml of
761 BHI broth containing 10 µg/ml tetracycline was inoculated with a single colony and genomic DNA
762 was extracted (Wizard DNA extraction kit, Promega). Genomic DNA was sequenced by paired-end

bioRxiv preprint doi: https://doi.org/10.1101/2021.02.12.430937; this version posted February 12, 2021. The copyright holder for this preprint (which was not certified by peer review) is the author/funder. All rights reserved. No reuse allowed without permission.

763 joining Illumina (Biomics Platform of the Institut Pasteur, Paris, France). Identification of the
764 mutations was performed with the *breseq* pipeline (Deatherage and Barrick, 2014).
765
766 **Plating efficiency assay.** Bacteria were grown to the late exponential phase*, i.e.* to an optical
767 density at 600 nm (OD_{600}) greater than 1.0 (*ca*. 6 h at 37 °C under agitation). The OD_{600} was
768 adjusted to 1.0 and 10-fold dilutions (10^{-1} to 10^{-6}) were prepared in BHI broth. Ten µl of the
769 resulting bacterial suspensions were spotted on BHI agar supplemented with inducers and drugs
770 as indicated in the legend to figures. For the disk diffusion assay, 5 µl of the bacterial suspension
771 adjusted to an OD_{600} of 1.0 were inoculated in 5 ml of water. BHI agar plates were flooded with
772 the latter suspension, excess liquid was removed, and the plates were kept at room temperature
773 for 15 min prior to the addition of paper disks containing antibiotics or inducers. Plates were
774 imaged after 16 h (or 24 h for plates containing ceftriaxone) of incubation at 37 °C.
775
776 **Purification of endopeptidases.** The *mepM* gene was amplified by PCR and cloned into pET-TEV
777 between the NdeI and XhoI restriction sites. The fusion protein comprised a 6 x histidine tag, a
778 TEV protease cleavage site, and residues 41-440 of MepM. The *mepH* and *mepS* genes were
779 independently amplified by PCR and cloned in frame with *dsbC* into pETMM82 using NEBuilder
780 HiFi DNA assembly (New England Biolabs). The fusion proteins comprised the DsbC chaperone
781 (Firczuk and Bochtler, 2007), a 6 x histidine tag, a TEV protease cleavage site, and residues 28-271
782 of MepH or 25-188 of MepS. The enzymes were produced in *E. coli* BL21(DE3) following induction
783 by 0.5 mM IPTG for 18 h at 16 ˚C. The endopeptidases were purified in 50 mM Tris-HCl pH 8.0
784 from a clarified lysate by nickel affinity chromatography (elution with 0.5 mM imidazole). The
785 endopeptidases were dialyzed overnight at 4 °C against 50 mM Tris-HCl pH 8.0, 0.5 mM EDTA. N-
786 terminal tags were cleaved overnight at room temperature following addition of 10 µg of TEV
787 protease for every mg of protein and DTT at a final concentration of 0.5 mM. MepM, MepH, and
788 MepS were further purified by size-exclusion chromatography (Superdex 75 HiLoad 26/60, GE
789 Healthcare) in 50 mM Tris-HCl pH 7.5, 200 mM NaCl.
790 PBP4 was purified from strain BL21(DE3) pET21bΩPBP4Δ1-60 as previously reported
791 (Banzhaf et al., 2020). Briefly, cells were grown in the presence of 1 mM IPTG for 8 h at 20 ^{o}C and

bioRxiv preprint doi: https://doi.org/10.1101/2021.02.12.430937; this version posted February 12, 2021. The copyright holder for this preprint (which was not certified by peer review) is the author/funder. All rights reserved. No reuse allowed without permission.

792 then harvested by centrifugation at 7,500 × *g*, 4 ^{o}C, 15 min. Cell pellets were resuspended in 50
793 mM Tris-HCl pH 8.0, 300 mM NaCl, and lysed by sonication. Following centrifugation at 14,000 ×
794 *g*, 1 h, 4 ^{o}C, the NaCl concentration was reduced by stepwise dialysis in a Spectra/Por dialysis
795 membrane (MWCO 12-14 kDa) against 50 mM Tris-HCl pH 8.5 containing (i) 200 mM NaCl, (ii) 100
796 mM NaCl, and (iii) 30 mM NaCl. The sample was centrifuged at 7,500 × *g*, 4 ^{o}C, 10 min and the
797 supernatant applied to a 5 ml HiTrap Q HP IEX column in 25 mM Tris-HCl pH 8.5, 30 mM NaCl.
798 Protein was eluted from the column with a linear gradient from 50 mM Tris-HCl pH 8.5, 100 mM
799 NaCl, to 25 mM Tris-HCl pH 8.0, 1 M NaCl, over a 100 ml volume. Fractions containing PBP4 were
800 combined and dialyzed against 10 mM potassium phosphate pH 6.8, 300 mM NaCl. Protein was
801 applied at 1 ml/min to a 5 ml ceramic hydroxyapatite column (BioRad BioscaleTM) in the dialysis
802 buffer, and a 50 ml linear gradient to 500 mM potassium phosphate pH 6.8, 300 mM NaCl, was
803 applied. Fractions with PBP4 were dialyzed overnight against 25 mM HEPES-NaOH pH 7.5, 300
804 mM NaCl, 10% glycerol, and concentrated to *ca.* 5 ml using a Vivaspin concentrator spin column
805 (Sartorius). The protein sample was applied to a HiLoad 16/600 Superdex 200 column (GE
806 healthcare) at 1 ml/min and eluted in a linear gradient to 25 mM HEPES-NaOH pH 7.5, 300 mM
807 NaCl, 10% glycerol. The collected fractions containing PBP4 were combined.

808 PBP7 was purified from strain BL21(DE3) pET28aΩ*pbpG*Δ1-75 as previously reported
809 (Banzhaf et al., 2020). Briefly, cells were grown in the presence of 1 mM IPTG for 3 h at 30 ^{o}C
810 before being harvested by centrifugation and resuspended in 25 mM Tris-HCl pH 7.5, 500 mM
811 NaCl, 20 mM imidazole. Following sonication and subsequent centrifugation, the lysate was
812 applied to a 5 ml HisTrap HP column (GE healthcare) and washed with 4 column volumes of 25
813 mM Tris-HCl pH 7.5, 500 mM NaCl, 20 mM imidazole. Bound protein was eluted with 25 mM Tris-
814 HCl pH 7.5, 300 mM NaCl, 400 mM Imidazole. Elution fractions containing PBP7 were combined
815 and dialyzed overnight against 25 mM HEPES-NaOH pH 7.5, 300 mM NaCl, 10% glycerol, in the
816 presence of 1 unit/ml of restriction grade thrombin (Novagen) to remove the oligohistidine tag.
817 The sample was then concentrated to *ca.* 5 ml using a Vivaspin concentrator spin column
818 (Sartorius) at 4,500 × *g*, 4 ^{o}C. The protein sample was applied to a HiLoad 16/600 Superdex 200
819 column (GE healthcare) at 1 ml/min and eluted in 25 mM HEPES-NaOH pH 7.5, 300 mM NaCl, 10%
820 glycerol. Elution fractions containing PBP7 were combined.

bioRxiv preprint doi: https://doi.org/10.1101/2021.02.12.430937; this version posted February 12, 2021. The copyright holder for this preprint (which was not certified by peer review) is the author/funder. All rights reserved. No reuse allowed without permission.

821 Protein concentrations were determined by the Bio-Rad protein assay using bovine serum
822 albumin as a standard. Endopeptidases were stored at -80 °C.
823
824 **Preparation of sacculi.** Bacteria were grown in M9 minimal medium supplemented with 0.1%
825 glucose at 37 °C for 48 h. Bacteria were harvested by centrifugation and boiled in 4% sodium
826 dodecyl sulfate (SDS) for 1 h. Sacculi were harvested by centrifugation (20,000 x *g* for 20 min at
827 20 °C), washed five times with water, and incubated with 100 µg/ml pronase overnight at 37 °C
828 in 20 mM Tris-HCl pH 7.5. Sacculi were washed five times with water and incubated overnight at
829 37 °C with 100 µg/ml trypsin in 20 mM sodium phosphate pH 8.0. Sacculi were washed five times
830 with water, boiled for 5 min, collected by centrifugation, resuspended in water, and stored at -20
831 °C.
832
833 **Digestion of sacculi.** Sacculi were digested overnight at 37 °C with 120 µM lysozyme alone or in
834 association with an endopeptidase in 40 mM Tris-HCl pH 8.0. Insoluble material was removed by
835 centrifugation and the soluble fraction containing muropeptides was reduced with sodium
836 borohydride for 1 h in 125 mM borate buffer pH 9.0. The pH of the solution containing the
837 reduced muropeptides was adjusted to 4.0 with phosphoric acid. Muropeptides were separated
838 by *rp*HPLC in a C18 column (Hypersil GOLD aQ; 250 x 4.6 mm; 3 µm, Thermoscientific) at a flow
839 rate of 1 ml/min with a linear gradient (0 to 20%) applied between 10 and 60 min (buffer A, TFA
840 0.1%; buffer B, acetonitrile 20% TFA 0.1%). Absorbance was monitored at 205 nm and fractions
841 were collected, lyophilized, and analyzed by mass spectrometry. Mass spectra were obtained on
842 a Bruker Daltonics maXis high-resolution mass spectrometer (Bremen, Germany) operating in the
843 positive mode (Analytical Platform of the Muséum National d'Histoire Naturelle, Paris, France).
844
845

Table S1. Characteristics and origin of the plasmids used in this study

Plasmid	Characteristics				Origin
Vectors					
pHV6	Tet^R	P_{trc}	*lacI*	*oriV* CloDF13	This study
pHV7	Cm^R	P_{araBAD}	*araC*	*oriV* P15a	This study
pHV9	Zeo^R	P_{phlF}	*phlF*	*oriV* pBR322	This study
pHV30	Zeo^R	P_{rhaBAD} TIS1	*rhaSR*	*oriV* pSC101	This study

bioRxiv preprint doi: https://doi.org/10.1101/2021.02.12.430937; this version posted February 12, 2021. The copyright holder for this preprint (which was not certified by peer review) is the author/funder. All rights reserved. No reuse allowed without permission.

pET-TEV	Km^R	P_{T7}	*lacI*	*oriV* ColE1	(Houben et al., 2007)
pETMM82	Km^R	P_{T7} *dsbC*	*lacI*	*oriV* ColE1	(Firczuk and Bochtler, 2007)
Recombinant plasmids for ycbB and relA' expression					
pKT2	pHV6Ω*ycbB*				(Hugonnet et al., 2016)
pKT8	pHV7Ω*relA'*				(Hugonnet et al., 2016)
pHV63	pHV7Ω*ycbB*				This study
Recombinant plasmids for complementation of endopeptidase gene deletions					
pHV10.1	pHV9Ω*mepM*				This study
pHV10.2	pHV9Ω*mepM* $H^{393}A$				This study
pHV10.3	pHV9Ω*mepM*Δ936-1224 (ΔLytM domain)				This study
pHV43.1	pHV30Ω*mepA*				This study
pHV43.2	pHV30Ω*mepA* $H^{113}A$				This study
pHV44	pHV30Ω*mepH*				This study
pHV45.1	pHV30Ω*mepK*				This study
pHV45.2	pHV30Ω*mepK* $H^{133}A$				This study
pHV46	pHV30Ω*mepM*				This study
pHV47.1	pHV30Ω*mepS*				This study
pHV47.2	pHV30Ω*mepS* $C^{94}A$				This study
pHV48	pHV30Ω*dacB*				This study
pHV49	pHV30Ω*pbpG*				This study
pHV50	pHV30Ω*ampH*				This study
pHV53	pHV30ΩTIS2-*mepM*				This study
pHV55	pHV7Ω*mepA*				This study
pHV56	pHV7Ω*mepH*				This study
pHV57	pHV7Ω*mepK*				This study
pHV58	pHV7Ω*mepM*				This study
pHV59	pHV7Ω*mepS*				This study
pHV60	pHV7Ω*dacB*				This study
pHV61	pHV7Ω*pbpG*				This study
pHV62	pHV7Ω*ampH*				This study
Recombinant plasmids for protein production					
pET-TEVΩ*mepM*Δ1-120	Production of MepM Δ1-40				This study
pETMM82Ω*mepH*Δ1-81	Production of MepH Δ1-27				This study
pETMM82Ω*mepS*Δ1-72	Production of MepS Δ1-24				This study
pET21bΩ*dacB*Δ1-60	Production of PBP4 Δ1-20				Banzhaf *et al.*, 2020
pET28aΩ*pbpG*Δ1-75	Production of PBP7 Δ1-25				Banzhaf *et al.*, 2020

846

Table S2. Characteristics and origin of *E. coli* strains used in this study

Strain	**Characteristics**	**Origin**
BW25113	Δ(*araD-araB*)*567* Δ(*rhaD-rhaB*)*568* Δ*lacZ4787* (::rrnB-3) *hsdR514 rph-1*	(Baba et al., 2006)
BW25113(*ycbB, relA'*)	Δ*relA* derivative of BW25113 harboring pKT2(*ycbB*) and pKT8(*relA'*)	(Hugonnet et al., 2016)
BW25113 M1	Ampicillin resistant derivative of BW25113 pJEH12(*ycbB*) harboring a mutation in the 5' UTR region of *ileRS*	(Hugonnet et al., 2016)
BL21(DE3)	Host for protein production	(Wood, 1966)

bioRxiv preprint doi: https://doi.org/10.1101/2021.02.12.430937; this version posted February 12, 2021. The copyright holder for this preprint (which was not certified by peer review) is the author/funder. All rights reserved. No reuse allowed without permission.

847

848 **ACKNOWLEDGEMENTS**

849 This work was supported by the French National Research Agency ANR 'RegOPeps' (grant ANR-
850 19-CE44-0007 to JEH). We thank L. Dubost and A. Marie for technical assistance in the collection
851 of mass spectra. We also thank L. Ma and R. Legendre for technical assistance in genome
852 sequencing. The Biomics Platform is a member of the 'France Génomique' consortium supported
853 by the French National Research Agency ANR (grant ANR-10-INBS-0009) and IBISA. We also thank
854 Z. Edoo for proofreading the manuscript.

855

856 **COMPETING INTEREST**

857 The authors declare that there is no conflict of interest.

858

859 **REFERENCES**

860 Baba T, Ara T, Hasegawa M, Takai Y, Okumura Y, Baba M, Datsenko KA, Tomita M, Wanner BL, Mori H.
861 2006. Construction of *Escherichia coli* K-12 in-frame, single-gene knockout mutants: the Keio
862 collection. *Mol Syst Biol* **2**. doi:10.1038/msb4100050

863 Banzhaf M, Yau HC, Verheul J, Lodge A, Kritikos G, Mateus A, Cordier B, Hov AK, Stein F, Wartel M, Pazos
864 M, Solovyova AS, Breukink E, van Teeffelen S, Savitski MM, den Blaauwen T, Typas A, Vollmer W.
865 2020. Outer membrane lipoprotein NlpI scaffolds peptidoglycan hydrolases within multi-enzyme
866 complexes in *Escherichia coli*. *EMBO J* **39**. doi:10.15252/embj.2019102246

867 Baranowski C, Welsh MA, Sham L-T, Eskandarian HA, Lim HC, Kieser KJ, Wagner JC, McKinney JD, Fantner
868 GE, Ioerger TR, Walker S, Bernhardt TG, Rubin EJ, Rego EH. 2018. Maturing *Mycobacterium*
869 *smegmatis* peptidoglycan requires non-canonical crosslinks to maintain shape. *Elife* **7**.
870 doi:10.7554/eLife.37516

871 Bastos PAD, Wheeler R, Boneca IG. 2020. Uptake, recognition and responses to peptidoglycan in the
872 mammalian host. *FEMS Microbiol Rev* **45**. doi:10.1093/femsre/fuaa044

873 Caveney NA, Caballero G, Voedts H, Niciforovic A, Worrall LJ, Vuckovic M, Fonvielle M, Hugonnet J-E,
874 Arthur M, Strynadka NCJ. 2019. Structural insight into YcbB-mediated beta-lactam resistance in
875 *Escherichia coli*. *Nat Commun* **10**:1849. doi:10.1038/s41467-019-09507-0

876 Cho H, Uehara T, Bernhardt TG. 2014. Beta-Lactam Antibiotics Induce a Lethal Malfunctioning of the
877 Bacterial Cell Wall Synthesis Machinery. *Cell* **159**:1300–1311. doi:10.1016/j.cell.2014.11.017

878 Chodisetti PK, Reddy M. 2019. Peptidoglycan hydrolase of an unusual cross-link cleavage specificity
879 contributes to bacterial cell wall synthesis. *Proc Natl Acad Sci* **116**:7825–7830.

bioRxiv preprint doi: https://doi.org/10.1101/2021.02.12.430937; this version posted February 12, 2021. The copyright holder for this preprint (which was not certified by peer review) is the author/funder. All rights reserved. No reuse allowed without permission.

880 doi:10.1073/pnas.1816893116

881 Datsenko KA, Wanner BL. 2000. One-step inactivation of chromosomal genes in *Escherichia coli* K-12
882 using PCR products. *Proc Natl Acad Sci U S A* **97**:6640–6645. doi:10.1073/pnas.120163297

883 Deatherage DE, Barrick JE. 2014. Identification of mutations in laboratory-evolved microbes from next-
884 generation sequencing data using *breseq*. *Methods Mol Biol* **1151**:165–188. doi:10.1007/978-1-
885 4939-0554-6_12

886 Delhaye A, Collet JF, Laloux G. 2016. Fine-tuning of the Cpx envelope stress response is required for cell
887 wall homeostasis in *Escherichia coli*. *MBio* **7**:47–63. doi:10.1128/mBio.00047-16

888 Denome SA, Elf PK, Henderson TA, Nelson DE, Young KD. 1999. *Escherichia coli* mutants lacking all
889 possible combinations of eight penicillin binding proteins: Viability, characteristics, and implications
890 for peptidoglycan synthesis. *J Bacteriol* **181**:3981–3993. doi:10.1128/jb.181.13.3981-3993.1999

891 Elowitz MB, Leibler S. 2000. A synthetic oscillatory network of transcriptional regulators. *Nature*
892 **403**:335–8. doi:10.1038/35002125

893 Engel H, van Leeuwen AM, Dijkstra A, Keck W. 1992. Enzymatic preparation of 1,6-anhydro-
894 muropeptides by immobilized murein hydrolases from *Escherichia coli* fused to staphylococcal
895 protein A. *Appl Microbiol Biotechnol* **37**:772–783. doi:10.1007/BF00174845

896 Firczuk M, Bochtler M. 2007. Mutational analysis of peptidoglycan amidase MepA. *Biochemistry* **46**:120–
897 128. doi:10.1021/bi0613776

898 Glauner B, Holtje J V., Schwarz U. 1988. The composition of the murein of *Escherichia coli*. *J Biol Chem*
899 **263**:10088–10095.

900 Gonzalez-Leiza SM, de Pedro MA, Ayala JA. 2011. AmpH, a Bifunctional DD-Endopeptidase and DD-
901 Carboxypeptidase of *Escherichia coli*. *J Bacteriol* **193**:6887–6894. doi:10.1128/JB.05764-11

902 Hecht A, Glasgow J, Jaschke PR, Bawazer LA, Munson MS, Cochran JR, Endy D, Salit M. 2017.
903 Measurements of translation initiation from all 64 codons in *E. coli*. *Nucleic Acids Res* **45**:3615–
904 3626. doi:10.1093/nar/gkx070

905 Heidrich C, Ursinus A, Berger J, Schwarz H, Höltje JV. 2002. Effects of multiple deletions of murein
906 hydrolases on viability, septum cleavage, and sensitivity to large toxic molecules in *Escherichia coli*.
907 *J Bacteriol* **184**:6093–6099. doi:10.1128/JB.184.22.6093-6099.2002

908 Henderson TA, Young KD, Denome SA, Elf PK. 1997. AmpC and AmpH, proteins related to the class C
909 beta-lactamases, bind penicillin and contribute to the normal morphology of *Escherichia coli*. *J*
910 *Bacteriol* **179**:6112–21. doi:10.1128/jb.179.19.6112-6121.1997

911 Höltje J V, Heidrich C. 2001. Enzymology of elongation and constriction of the murein sacculus of
912 *Escherichia coli*. *Biochimie* **83**:103–8. doi:10.1016/s0300-9084(00)01226-8

913 Houben K, Marion D, Tarbouriech N, Ruigrok RWH, Blanchard L. 2007. Interaction of the C-Terminal
914 Domains of Sendai Virus N and P Proteins: Comparison of Polymerase-Nucleocapsid Interactions
915 within the Paramyxovirus Family. *J Virol* **81**:6807–6816. doi:10.1128/jvi.00338-07

916 Hugonnet JE, Mengin-Lecreulx D, Monton A, den Blaauwen T, Carbonnelle E, Veckerlé C, Yves VB, van
917 Nieuwenhze M, Bouchier C, Tu K, Rice LB, Arthur M. 2016. Factors essential for L,D-transpeptidase-
918 mediated peptidoglycan cross-linking and β-lactam resistance in *Escherichia coli*. *Elife* **5**.

bioRxiv preprint doi: https://doi.org/10.1101/2021.02.12.430937; this version posted February 12, 2021. The copyright holder for this preprint (which was not certified by peer review) is the author/funder. All rights reserved. No reuse allowed without permission.

919 doi:10.7554/eLife.19469

920 Johnson JW, Fisher JF, Mobashery S. 2013. Bacterial cell-wall recycling. *Ann N Y Acad Sci* **1277**:54–75.
921 doi:10.1111/j.1749-6632.2012.06813.x

922 Keck W, Schwarz U. 1979. *Escherichia coli* murein-DD-endopeptidase insensitive to beta-lactam
923 antibiotics. *J Bacteriol* **139**:770–4.

924 Kocaoglu O, Carlson EE. 2015. Profiling of β-lactam selectivity for penicillin-binding proteins in
925 *Escherichia coli* strain DC2. *Antimicrob Agents Chemother* **59**:2785–2790. doi:10.1128/AAC.04552-
926 14

927 Korat B, Mottl H, Keck W. 1991. Penicillin-binding protein 4 of *Escherichia coli*: molecular cloning of the
928 *dacB* gene, controlled overexpression, and alterations in murein composition. *Mol Microbiol* **5**:675–
929 684. doi:10.1111/j.1365-2958.1991.tb00739.x

930 Lai GC, Cho H, Bernhardt TG. 2017. The mecillinam resistome reveals a role for peptidoglycan
931 endopeptidases in stimulating cell wall synthesis in *Escherichia coli*. *PLOS Genet* **13**:e1006934.
932 doi:10.1371/journal.pgen.1006934

933 Magnet S, Dubost L, Marie A, Arthur M, Gutmann L. 2008. Identification of the L,D-Transpeptidases for
934 Peptidoglycan Cross-Linking in *Escherichia coli*. *J Bacteriol* **190**:4782–4785. doi:10.1128/JB.00025-08

935 Mainardi JL, Fourgeaud M, Hugonnet JE, Dubost L, Brouard JP, Ouazzani J, Rice LB, Gutmann L, Arthur M.
936 2005. A novel peptidoglycan cross-linking enzyme for a β-lactam-resistant transpeptidation
937 pathway. *J Biol Chem* **280**:38146–38152. doi:10.1074/jbc.M507384200

938 Mainardi JL, Villet R, Bugg TD, Mayer C, Arthur M. 2008. Evolution of peptidoglycan biosynthesis under
939 the selective pressure of antibiotics in Gram-positive bacteria. *FEMS Microbiol Rev*.
940 doi:10.1111/j.1574-6976.2007.00097.x

941 Morè N, Martorana AM, Biboy J, Otten C, Winkle M, Serrano CKG, Montón Silva A, Atkinson L, Yau H,
942 Breukink E, den Blaauwen T, Vollmer W, Polissi A. 2019. Peptidoglycan Remodeling Enables
943 *Escherichia coli* To Survive Severe Outer Membrane Assembly Defect. *MBio* **10**.
944 doi:10.1128/mBio.02729-18

945 Pazos M, Peters K. 2019. Peptidoglycan. Subcellular Biochemistry. Springer New York. pp. 127–168.
946 doi:10.1007/978-3-030-18768-2_5

947 Pazos M, Peters K, Vollmer W. 2017. Robust peptidoglycan growth by dynamic and variable multi-protein
948 complexes. *Curr Opin Microbiol*. doi:10.1016/j.mib.2017.01.006

949 Pisabarro AG, De Pedro MA, Vazquez D. 1985. Structural modifications in the peptidoglycan of
950 *Escherichia coli* associated with changes in the state of growth of the culture. *J Bacteriol* **161**:238–
951 242. doi:10.1128/jb.161.1.238-242.1985

952 Ringquist S, Shinedling S, Barrick D, Green L, Binkley J, Stormo GD, Gold L. 1992. Translation initiation in
953 *Escherichia coli*: sequences within the ribosome-binding site. *Mol Microbiol* **6**:1219–1229.
954 doi:10.1111/j.1365-2958.1992.tb01561.x

955 Romeis T, Holtje J-V. 1994. Penicillin-binding Protein 7/8 of *Escherichia coli* is a DD-endopeptidase. *Eur J*
956 *Biochem* **224**:597–604. doi:10.1111/j.1432-1033.1994.00597.x

957 Sanders AN, Pavelka MS. 2013. Phenotypic analysis of *Eschericia coli* mutants lacking L,D-

bioRxiv preprint doi: https://doi.org/10.1101/2021.02.12.430937; this version posted February 12, 2021. The copyright holder for this preprint (which was not certified by peer review) is the author/funder. All rights reserved. No reuse allowed without permission.

958 transpeptidases. *Microbiology* **159**:1842–1852. doi:10.1099/mic.0.069211-0

959 Sauvage E, Kerff F, Terrak M, Ayala JA, Charlier P. 2008. The penicillin-binding proteins: Structure and
960 role in peptidoglycan biosynthesis. *FEMS Microbiol Rev*. doi:10.1111/j.1574-6976.2008.00105.x

961 Schreiber G, Metzger S, Aizenman E, Roza S, Cashel M, Glaser G. 1991. Overexpression of the *relA* gene in
962 *Escherichia coli*. *J Biol Chem* **266**:3760–3767. doi:10.1016/s0021-9258(19)67860-9

963 Singh SK, Parveen S, SaiSree L, Reddy M. 2015. Regulated proteolysis of a cross-link–specific
964 peptidoglycan hydrolase contributes to bacterial morphogenesis. *Proc Natl Acad Sci* **112**:10956–
965 10961. doi:10.1073/pnas.1507760112

966 Singh SK, SaiSree L, Amrutha RN, Reddy M. 2012. Three redundant murein endopeptidases catalyse an
967 essential cleavage step in peptidoglycan synthesis of *Escherichia coli* K12. *Mol Microbiol* **86**:1036–
968 1051. doi:10.1111/mmi.12058

969 Truong TT, Vettiger A, Bernhardt TG. 2020. Cell division is antagonized by the activity of peptidoglycan
970 endopeptidases that promote cell elongation. *Mol Microbiol* **114**:966–978. doi:10.1111/mmi.14587

971 Turner RD, Vollmer W, Foster SJ. 2014. Different walls for rods and balls: the diversity of peptidoglycan.
972 *Mol Microbiol* **91**:862–874. doi:10.1111/mmi.12513

973 Uehara T, Dinh T, Bernhardt TG. 2009. LytM-domain factors are required for daughter cell separation and
974 rapid ampicillin-induced lysis in *Escherichia coli*. *J Bacteriol* **191**:5094–5107. doi:10.1128/JB.00505-
975 09

976 Uehara T, Park JT. 2008. Growth of *Escherichia coli*: Significance of peptidoglycan degradation during
977 elongation and septation. *J Bacteriol* **190**:3914–3922. doi:10.1128/JB.00207-08

978 van Heijenoort J. 2011. Peptidoglycan Hydrolases of *Escherichia coli*. *Microbiol Mol Biol Rev* **75**:636–663.
979 doi:10.1128/mmbr.00022-11

980 Vellanoweth RL, Rabinowitz JC. 1992. The influence of ribosome-binding-site elements on translational
981 efficiency in *Bacillus subtilis* and *Escherichia coli* in vivo. *Mol Microbiol* **6**:1105–1114.
982 doi:10.1111/j.1365-2958.1992.tb01548.x

983 Verheul J, Lodge A, Yau HC, Liu X, Typas A, Banzhaf M, Vollmer W, den T. 2020. Midcell localization of
984 PBP4 of *Escherichia coli* is essential for the timing of divisome assembly. *bioRxiv*
985 2020.07.30.230052. doi:10.1101/2020.07.30.230052

986 Vollmer W. 2012. Bacterial growth does require peptidoglycan hydrolases. *Mol Microbiol* **86**:1031–1035.
987 doi:10.1111/mmi.12059

988 Weber H, Polen T, Heuveling J, Wendisch VF, Hengge R. 2005. Genome-wide analysis of the general
989 stress response network in *Escherichia coli*: σS-dependent genes, promoters, and sigma factor
990 selectivity. *J Bacteriol* **187**:1591–1603. doi:10.1128/JB.187.5.1591-1603.2005

991 Wood WB. 1966. Host specificity of DNA produced by *Escherichia coli*: Bacterial mutations affecting the
992 restriction and modification of DNA. *J Mol Biol* **16**:118–133. doi:10.1016/S0022-2836(66)80267-X

993